

Published in final edited form as:

*Nano Today*. 2015 February 1; 10(1): 93–117. doi:10.1016/j.nantod.2015.01.005.

## Core-Crosslinked Polymeric Micelles: Principles, Preparation, Biomedical Applications and Clinical Translation

Marina Talelli<sup>#1,2</sup>, Matthias Barz<sup>#3</sup>, Cristianne J. Rijcken<sup>4</sup>, Fabian Kiessling<sup>5</sup>, Wim E. Hennink<sup>1</sup>, and Twan Lammers<sup>1,5,6,\*</sup>

<sup>1</sup>Department of Pharmaceutics, Utrecht Institute for Pharmaceutical Sciences, Utrecht University, Utrecht, The Netherlands <sup>2</sup>Department of Immunology and Oncology and NanoBiomedicine Initiative, Centro Nacional de Biotecnología (CNB)/CSIC, Darwin 3, Cantoblanco, 28049 Madrid, Spain <sup>3</sup>Institute of Organic Chemistry, Johannes Gutenberg-University Mainz, Duesbergweg 10-14, 55128 Mainz, Germany <sup>4</sup>Cristal Therapeutics, Oxfordlaan 55, 6229 EV Maastricht, the Netherlands <sup>5</sup>Department of Nanomedicine and Theranostics, Institute for Experimental Molecular Imaging, University Clinic and Helmholtz Institute for Biomedical Engineering, RWTH Aachen University, Aachen, Germany <sup>6</sup>Department of Controlled Drug Delivery, University of Twente and MIRA Institute for Biomedical Technology and Technical Medicine, Enschede, The Netherlands

# These authors contributed equally to this work.

### Abstract

Polymeric micelles (PM) are extensively used to improve the delivery of hydrophobic drugs. Many different PM have been designed and evaluated over the years, and some of them have steadily progressed through clinical trials. Increasing evidence suggests, however, that for prolonged circulation times and for efficient EPR-mediated drug targeting to tumors and to sites of inflammation, PM need to be stabilized, to prevent premature disintegration. Core-crosslinking is among the most popular methods to improve the *in vivo* stability of PM, and a number of core-crosslinked polymeric micelles (CCPM) have demonstrated promising efficacy in animal models. The latter is particularly true for CCPM in which (pro-) drugs are covalently entrapped. This ensures proper drug retention in the micelles during systemic circulation, efficient drug delivery to pathological sites via EPR, and tailorable drug release kinetics at the target site. We here summarize recent advances in the CCPM field, addressing the chemistry involved in preparing them, their *in vitro* and *in vivo* performance, potential biomedical applications, and guidelines for efficient clinical translation.

### Keywords

Nanomedicine; Drug targeting; EPR; Micelle; Polymer; Core-crosslinking

---

\*Corresponding author: Prof. Twan Lammers, RWTH Aachen University Clinic, Pauwelsstrasse 30, 52074 Aachen, Germany. tlammers@ukaachen.de. Tel: +49-2418036681. Fax: +49-241803380116.

## 1. Introduction

In the last 2-3 decades, nanomedicines have started to attract significant attention. Both at the academic and at the industrial level, an ever-increasing number of scientists are working on the development of 1-100(0) nm-sized drug delivery systems. This increasing interest in nanomedicine research is on the one hand based on the continuing progress made in the fields of nanotechnology, polymer chemistry and chemical engineering, giving rise to an ever increasing number of nanomaterials that can - in principle - be used for drug delivery purposes [1-5]. On the other hand, in spite of many years of drug delivery research, there still are many drug molecules (in particular highly hydrophobic compounds, proteins and nucleic acids) and diseases (in particular cancer) which require further improvements in delivery, to really improve therapeutic outcome and the quality of life of patients [6-9].

Chemotherapeutic drugs are an excellent example to demonstrate the need for improved delivery. *In vitro*, i.e. in cell culture, chemotherapeutic agents are often highly potent, killing the vast majority of cancer cells at pico- to micromolar concentrations. In animal models and in patients, on the other hand, they generally fail to provide sufficient therapeutic efficacy. This failure is likely mostly due to inefficient accumulation and insufficient retention at the target site, resulting in suboptimal therapeutic responses. At the same time, significant amounts of intravenously (i.v.) administered chemotherapeutic drugs accumulate in healthy tissues, causing serious side effects and therefore lowering the quality of life of patients. These deleterious pharmacokinetic and biodistributional properties result from a number of chemical, anatomical, biological and physiological barriers [10-12]. Among the most important (physico-) chemical barriers are the low molecular weight, low solubility, low stability and high hydrophobicity of anticancer agents. These parameters generally lead to short circulation times upon i.v. injection, with only a small percentage of the i.v. injected dose (%ID) eventually reaching the target site. In addition, they result in a relatively large volume of distribution, causing chemotherapeutic drugs to accumulate in several different healthy organs.

By entrapping chemotherapeutic drugs in liposomes or micelles, or by conjugating them to water-soluble polymers or proteins, the apparent molecular weight of the agents increases, and their volume of distribution decreases. The latter attenuates their accumulation in healthy tissues, while the former increases their circulation times, and by means of the Enhanced Permeability and Retention (EPR) effect, enables them to accumulate in tumors more efficiently. The EPR effect has been described by Maeda and colleagues ~30 years ago, and it is based on the notion that cancerous (and inflamed) tissues possess leaky blood vessels, allowing for the extravasation of nanomaterials with sizes of up to several hundreds of nanometers, while at the same time promoting their retention at the pathological site because of defective lymphatic drainage [13, 14].

Many different nanomedicines have been designed and evaluated over the years [2-9, 12, 15-19]. The (pre-) clinically most relevant formulations are depicted in Figure 1, and virtually all of them are designed to take advantage of the EPR effect. This implies that the key characteristics of nanomedicines are I) ensuring efficient, stable and reversible drug loading and II) enabling prolonged circulation times (as a prolonged circulation time

constitutes the basis for efficient EPR). Of particular importance in this regard is the development of systems that improve the administration and target site accumulation of highly hydrophobic drugs. In the case of cancer, for instance, taxane-based chemotherapeutics such as paclitaxel and docetaxel are known to be among the most potent drugs, and they are extensively employed in the clinic. However, because of their high hydrophobicity, their i.v. administration is problematic, requiring drop-wise infusion for multiple hours in relatively toxic (immunogenic) solubilisation enhancers, such as Cremophor. Thus, the co-administration of corticosteroids and anti-histaminics, to suppress infusion-related inflammatory and hypersensitivity reactions, is mandatory.

Nanomedicines hold significant potential for improving this situation, i.e. to substantially enhance the bioavailability of highly hydrophobic anticancer agents. This can be best exemplified by looking at Abraxane [20, 21]: by co-condensing paclitaxel with albumin, a 130 nm-sized nanoparticulate-formulation is obtained, which is administered to patients without the need for corticosteroid and anti-histaminic co-administration. Because of the increased tolerability profile, this albumin-based paclitaxel formulation enables the administration of higher doses (175 mg/m<sup>2</sup> for Taxol (i.e. paclitaxel in Cremophor) vs. 225 mg/m<sup>2</sup> for Abraxane), which likely explains the improved patients responses observed in phase III clinical trials [22]. However, it has to be kept in mind in this regard that although Abraxane is a nanomedicine formulation, it disintegrates almost immediately upon i.v. injection, as demonstrated by an equal pharmacokinetic profile as compared to Taxol, with paclitaxel being transferred to endogenous albumin (as in the case of Taxol). Consequently, Abraxane does not provide improved circulation times as compared to Taxol, and therefore does not exploit the EPR effect to result in higher tumor concentrations [23, 24].

Because of their physicochemical nature, consisting of a hydrophobic core and a hydrophilic shell, polymeric micelles (PM) are highly suited for enabling EPR-mediated passive drug targeting of hydrophobic compounds [25-32]. PM are based on amphiphilic block-copolymers, which can self-assemble into well-defined core-shell-structures at concentrations exceeding their critical micelle concentration (CMC). Their low-molecular-weight counterparts, i.e. surfactant-based micelles, exhibit significantly higher critical micelle concentrations (CMCs), leading to reduced stability as compared to PM, as well as a number of side effects. For example, Cremophor EL<sup>®</sup> (i.e. polyoxyethylated fatty acid) is biologically and pharmacologically active, and it also leaches plasticizers from standard i.v. tubing material, e.g. di(2-ethylhexyl)phthalate (DEHP) [33]. In addition, Cremophor infusion induces histamine release and a number of hypersensitivity reactions, such as anaphylaxis [34]. Therefore, PM have attracted a lot of attention in the last couple of years, as they possess much lower CMCs, and consequently are highly useful for solubilizing and stabilizing hydrophobic compounds, leading to prolonged circulation times and to increased target site accumulation, and thereby to improved therapeutic indices [35-37].

However, when applied *in vivo*, conventional micellar nanomedicines face several difficulties, primarily related to their premature disintegration in systemic circulation [38]. This can be caused both by dilution in the bloodstream as well as by interactions of the micellar building blocks (unimers) with blood components (in particular plasma proteins; such as albumin and apolipoproteins), which shifts the micellar equilibrium toward the

unimer state. As a result of this, the vast majority of (pre-) clinically used micellar nanomedicines have thus far not managed to demonstrate significant improvements in circulation times, target site accumulation and therapeutic efficacy [39, 40].

A simple and straightforward strategy to overcome the premature disintegration of micellar nanomedicines to stabilize them via crosslinking, to thereby assure prolonged circulation times and efficient EPR-mediated target site accumulation. In this approach, the assembly of the unimers is not only based on hydrophobic interactions, but is also stabilized via the formation of crosslinks either in the core or in the corona of the micelles. These crosslinks can e.g. be based on covalent bonds, hydrogen bonding or  $\pi$ - $\pi$ -stacking. However, although the pharmacokinetic properties of PM tend to be significantly improved upon crosslinking, the same generally does not hold true for physically (i.e. non-covalently) entrapped drugs. These tend to diffuse out of the micellar core very rapidly (because of entropy gain), almost regardless of core-crosslinking, and they are consequently cleared from systemic circulation within minutes to hours [38, 41, 42]. Moreover, even if they are (semi-) stably entrapped in the micellar core, non-covalently entrapped drug molecules tend to be released from PM in a non-controlled manner, which is suboptimal for ensuring sustained and tailored release kinetics. To overcome these shortcomings, recent efforts in this area of research have moved towards the covalent attachment of (pro-) drug molecules in the micellar core, in order to ensure stable drug retention during systemic circulation, and to enable tailorable release kinetics, e.g. via the use of stimuli-responsive drug linkers, resulting in more specific and sustained drug release upon accumulation at the pathological site. An increasing number of such core-crosslinked PM containing covalently linked drugs has been designed and evaluated in the last couple of years, with very promising *in vivo* results, and several of these materials are currently entering early stage clinical evaluation.

In the present manuscript, we describe the principles and preparation of the most common types of core-crosslinked polymeric micelles (CCPM). In addition, using selected examples from the literature, we demonstrate that core-crosslinking and covalent drug attachment significantly improve the *in vivo* performance of PM, regarding not only biodistribution and target site accumulation, but also regarding therapeutic efficacy and tolerability. We finally also discuss the most important pharmaceutical, pharmacological and regulatory issues to keep in mind when intending to translate CCPM to the clinic. Together, the advances made and the insights obtained indicate that CCPM are highly interesting materials for systemic drug delivery, (i) facilitating the formulation and administration of highly hydrophobic (anticancer) agents; (ii) improving their *in vivo* stability and circulation time; (iii) increasing their target site accumulation; (iv) controlling their drug release kinetics; (v) enhancing their therapeutic efficacy; (vi) reducing their systemic side effects; and (vii) easing their administration.

## 2. Polymeric micelles

### 2.1. Principles

The International Union of Pure and Applied Chemistry (IUPAC) defines a micelle as “an aggregate of colloidal dimensions formed by surfactants in solutions, which exists in equilibrium with the molecules or ions from which they are formed” [43], and a polymeric

micelle is defined as “a micelle formed by one or more block or graft copolymers in a selective solvent”. An overview of the (pre-) clinically most relevant polymer-based core-shell self-assemblies and a description of their physicochemical properties is provided in Figure 2. In addition to the nano-self-assemblies described in Figure 2, a number of other and generally more complex block copolymer micelles have been described in literature, e.g. crew-cut micelles [44] as well as multi-compartment micelles (e.g. onion-like micelles) [45-47]. Here, we focus on standard PM and on core-crosslinked PM, as these systems have progressed most with regard to *in vivo* evaluation, biomedical application and clinical translation.

Polymeric micelles exhibit a radial density profile characteristic of a semi-dilute polymer solution confined to a spherical domain [1] and are in most cases spontaneously formed, when the unimer concentration reaches the critical micelle concentration (CMC) (figure 4A). The principles of the micellization of block copolymers, as well as their preparation, their dynamics and their physicochemical characterization have been studied for decades, and are well-described in the literature [52-55]. The typical core-shell structure of polymeric micelles appears highly suited for prolonged circulation times and EPR-mediated passive drug targeting to tumors and to inflammation sites, because it separates the bioactive agent in the core from the environment by a hydrophilic protective corona (which ideally is stealth-like). Efficient EPR- and micelle-mediated drug delivery can be tailored at several levels, e.g. by optimizing the chemical properties of the shell (i.e. stealth-like corona, active targeting, etc) and the core (i.e. optimized for drug encapsulation, enabling core-crosslinking, enabling covalent drug attachment, etc). The most convenient way to prepare such core-shell micellar nanocarriers is via the self-assembly of amphiphilic block copolymers in a block-selective solvent (usually in aqueous solutions). To facilitate micelle formation and ensure colloidal stability, the core-forming block needs to be highly hydrophobic, while the corona-forming block needs to be highly hydrophilic (non-ionic or zwitterionic). In other words, the Flory-Huggins polymer-polymer interaction parameter ( $\chi$ ) between both blocks and the solvent-polymer of the hydrophobic block needs to be positive, while the hydrophilic block needs to possess a positive solvent-polymer interaction parameter, which leads to an overall gain of Gibbs free energy. Many different block copolymers have been synthesized and evaluated for preparing PM for drug delivery over the years. Materials of various building blocks, molecular weights and dispersities have been developed for such purposes [56, 57]. In number of cases, also convincing proof-of-principle for improved *in vivo* circulation times, target site accumulation and therapeutic efficacy has been provided (see below).

## 2.2. Effect of polymer quality on PM properties

When preparing PM, the dispersity ( $\text{M}_w/\text{M}_n$ ; formerly known as polydispersity index (PDI)) of the block copolymer is an often under-appreciated factor influencing the shape, stability and overall performance of the final formulation. For example, a block copolymer with a number average molecular weight ( $\text{M}_n$ ) of 40 kg/mol and a dispersity of 1.04 has 99% of all macromolecules within the molecular weight range 20-60 kg/mol (Figure 3). However, this percentage steeply drops in the case of slightly higher dispersities, e.g. to 72% and 46% for

polymers with  $\sigma = 1.2$  or  $\sigma = 1.5$ , respectively (assuming a Gaussian normal distribution) [56].

Micellization is based on the phase-separation (demixing) of block copolymers in selected solvents, and this process depends on the polymer dispersity ( $\sigma$ ) [58]. Furthermore, the exchange kinetics of block copolymers between the micellar and the unimer state (and thus the stability of the micelles) are also influenced by the dispersity of the polymers [44], as the exchange dynamics of block copolymers in and out of micelles depend on the length of the hydrophobic block [59], as well as on the possible presence of hydrophobic homopolymer (side product in the synthesis of block copolymers by chain termination) [60]. Side reactions, such as chemical and physical chain termination, may also lead to undesired polymer properties, for example incomplete renal excretion due to high-molecular-weight impurities. Therefore, block copolymers with a low dispersity ( $\sigma < 1.2$ ) and a poisson-like molecular weight distribution are preferable for achieving either controlled self-assembly yielding well-ordered, relatively monodisperse core-shell structures and ensuring complete renal excretion for non-degradable materials.

In respect to this, the use of living (or controlled) polymerization methods, such as controlled ring opening polymerization or reversible-deactivation radical polymerization (NMP, ATRP or RAFT [61, 62]) are considered to be of high value [56]. These techniques are typical chain growth polymerizations, in which termination reactions are more or less efficiently suppressed. In contrast to conventional free radical polymerization or polycondensation techniques, these controlled chemical approaches offer various advantages. First of all, molecular weights can be controlled and adjusted to the desired needs. Second, since termination and side reactions in general are reduced (or even completely absent), block copolymers with a very narrow molecular weight distribution (i.e. low dispersity) can be obtained. And third, differences in copolymer microstructure are minimized, since polymer chains grow constantly and in a controlled manner. As opposed to free radical polymerization, which yields pseudo-homopolymers of the more reactive monomer in early stages and pseudo-homopolymers of the less reactive monomer at later stages, controlled polymerization techniques such as RAFT and ATRP yield more uniform gradient copolymers. Overall, synthetic polymer chemistry offers a plethora of well-defined polymeric architectures over a broad range of molecular weights. While PEG and some polypeptides are commercially available in various architectures, other polymers, like polyoxazolines [63], polypeptoides [64] and polyacrylates or polyacrylamides [56], can be synthesized fairly easily [56]. Future studies in which PM prepared using the same type of block copolymers but with lower dispersities are systematically compared appear rather interesting, to see how the dispersity influences the self-assembly and micelle properties *in vitro* as well as *in vivo*. Such studies can be expected to provide a proper framework for the more intense use of advanced polymerization techniques in nanomedicine research.

### 2.3. Clinical translation of first-generation PM

Up to date, a number of first-generation PM has entered clinical evaluation. The first enhancement of increased therapeutic efficacy of a drug using PM was published in 1989 [65], and since then a large number of formulations has been developed and entered clinical



trials [25, 26, 28, 66, 67] (see Table 1). One formulation has been approved (in Korea; GenexolPM), and a handful of others have progressed to Phase II/III trials (see Table 1). The main reason for this fairly efficient clinical translation is, as already alluded to above, the ability of PM to solubilize poorly soluble drugs, such as taxanes, thereby reducing or preventing the side effects typically associated with low- or intermediate-molecular-weight excipients (such as Cremophor or Tween). This is very important, as it is estimated that a great percentage of newly developed drugs have relatively poor aqueous solubility [66, 68].

However, in most cases the main challenge that PM face for their application *in vivo* is their instability in the circulation which results from the fact that PM (as also mentioned in their definition, Figure 2) are always in equilibrium with their unimers. Due to this dynamic nature, upon dilution after injection into the bloodstream the concentration of block copolymers decreases to levels below (or close to) the CMC, resulting in the disassembly of all or at least a high number of micelles. It should be underlined here that the CMC - by definition - does not only refer to the minimum concentration above which micelles are formed, but also to the maximum concentration of unimers that can be present in solution. This important notion and physicochemical fact is often not taken into account when visualizing, quantifying and explaining the biodistribution and target site accumulation of PM. There are always free unimers present in equilibrium with micelles and this fraction is often rapidly excreted renally and/or hepatobiliarly, or interacts unspecifically with plasma proteins. This results in their gradual removal from the micellar equilibrium, shifting it towards the unimer side, and eventual micelle dissociation, leading to uncontrollable biodistribution properties, as well as potential triggering of immune responses [84]. Therefore, although a low CMC surely is highly important, it is essential to keep in mind the nature of the free fraction of block copolymers that is always present in standard (i.e. non-crosslinked) PM, as this fraction might substantially affect several aspects of their *in vivo* performance (e.g. circulation time, clearance, target site accumulation, efficacy and toxicity).

Consequently, during the past years a lot of attention has been devoted to the factors that affect the PM stability, as well as on approaches to improve it [85]. The most popular and promising method of PM stabilization is their crosslinking, as the creation of stable crosslinks between the unimers preserves the micellar structure and therefore enables them to remain stable in the circulation upon i.v. injection, independent of dilution into large volumes and/or interaction with plasma proteins [42, 86, 87]. One of the first examples of this, showing substantially prolonged micelle half-life times in blood (>50 h), was reported by Rolland and colleagues in 1992 [88]. Crosslinking of PM is performed by the incorporation of stable bonds between unimers after micellar self-assembly. This can be done either on the outer or interfacial (triblock copolymer PM) part of PM [87, 89], or on their core [42, 86, 89]. Shell-crosslinking is an important method of stabilizing PM, but bears the risk of intermicellar crosslinking if not performed in high dilutions. In addition, the PM shell determines its surface and stealth properties, and its crosslinking might affect its hydrophilicity, and therefore also the PM circulation times. On the other hand, stabilization of PM by core-crosslinking is not expected to have an impact on the surface characteristics

of the PM, therefore neither on its stealth properties. Most importantly, the hydrophobic drugs physically encapsulated in CCPM can be attached to the cross-linkers of the core.

In the next sections, we focus on the methods of preparation of the most successful and clinically most advanced CCPM, and we showcase recent progress on their *in vitro* and *in vivo* performance. The advantages of covalently (and reversibly) encapsulating drugs in the crosslinked micellar core are also exemplified. The improved *in vivo* performance of CCPM as compared to non-crosslinked PM (NCPM) is clearly demonstrated, by means of improved pharmacokinetic and biodistributional profiles, as well as via improved *in vivo* efficacy.

### 3. Core-crosslinked polymeric micelles: Preparation

Covalent core-crosslinking is generally performed using PM consisting of side-chain or end-group-functionalized block copolymers, and it is always performed after micelle formation. Therefore, it is important that the reactive groups used for core-crosslinking do not interfere with the micellization process. This means that in the ideal case they have to be sufficiently hydrophobic or of low number to not disturb the formation of relatively homogenous and monodisperse micelles.

The most extensively employed methods for preparing core-crosslinked polymeric micelles are: I) radical polymerization, which is used for PM containing polymerizable groups within their core; II) the addition of a bifunctional crosslinker, which applies to PM containing reactive groups within their core; and III) disulphide bridges, in the case of PM containing thiol groups (Figure 4B). We have treated this last method of preparation of CCPM as a separate one, as it is a method in which the resulting crosslinks are intrinsically biodegradable in reducing environments, thus giving the option of stimuli-responsive disintegration and drug release.

Several other types of chemistries have also been employed and are described in section 3.1.4. As demonstrated in the subsequent sections, via these diverse methods of core-crosslinking, significant improvements in the circulation kinetics, the biodistribution and the target site accumulation of CCPM can be achieved, with much longer circulation times and with significantly increased drug concentrations localizing at the pathological site.

#### 3.1. Core-crosslinking of PM using radical polymerization

Radical polymerization (Figure 4B) is used when polymerizable groups are present in the core-forming block. Core-crosslinking is performed after micelle formation, either by photo-initiated polymerization or by the addition of free radical initiators. Below, several representative examples of the chemistries that have been employed thus far are provided.

Kataoka and colleagues synthesized 20-30 nm PM formed by amphiphilic poly(ethylene glycol)-b-poly(lactide) (PEG-b-PLA) block copolymers functionalized with methacrylate groups in the PLA core-forming block [90]. The PM were crosslinked via thermal free radical polymerization of the methacrylate groups, and they demonstrated increased stability as compared to non-crosslinked micelles upon treatment with SDS, as well as upon long-term storage. In a similar approach, 150-250 nm-sized micelles based on triblock



copolymers of (PLA-PEG-PLA) end modified with acrylate groups were crosslinked by UV illumination of a photo-initiator forming nanogels, which were shown to be significantly more stable than their non-crosslinked counterparts [91]. Kissel and coworkers performed similar studies using di- and triblock copolymers of PEG-PCL and PEG-PCL-PEG, in which PCL was functionalized with core-cross-linkable double bonds [92]. The 40-200 nm micelles (size depended on reaction conditions and copolymer composition) were core-crosslinked with  $K_2S_2O_8$  and presented good stability, even upon high dilution. As an example of thermally induced polymerization, micelles based on hydrophilic PEG and hydrophobic allyl containing poly[(L-lactide)-co-(5-methyl-5-allyloxycarbonyl-1,3-dioxan-2-one)] (p(LA-co-MAC)) were core-crosslinked via thermal polymerization using AIBN, resulting in ~120 nm-sized CCPM [93], which demonstrated increased stability upon long-term storage. Analogously, PM based on biodegradable block copolymers of poly(ethylene glycol)-hyperbranched poly( $\beta$ -aminoester)s with acrylate group terminals (PEG-HBPAE-A) were core-crosslinked by UV irradiation of a UV radical initiator, resulting in a significantly enhanced stability as compared to non-crosslinked micelles in serum-containing cell culture medium [94]. In this particular example, a pH-dependent release of doxorubicin (DOX) from the CCPM was observed, being fast at pH 5 and slow at pH 7.4, attributed to core-swelling of the CCPM at acidic pH (due to the protonation of the tertiary amines in the core). Using real-time fluorescence microscopy, the in-situ uptake of DOX-loaded CCPM by MCF-7 cells was monitored, and it was observed that over time, the DOX fluorescence became more intense (indicative of release; via dequenching) [94]. At the same time, the cells changed their morphology from stretched to round, with a clearly shrunk cytoplasm and a clearly swollen nucleus, pointing toward the induction of programmed cell death. Another example of pH responsive CCPM was recently reported by Wu et al [95]. In this study, diblock copolymers based on poly(ethylene glycol)-*b*-poly(mono-2,4,6-trimethoxy benzylidene-pentaerythritol carbonate-co-acryloyl carbonate) (PEG-*b*-P(TMBPEC-co-AC)) were used to form PM and core-crosslinked using the acryloyl groups in the polycarbonate block by UV irradiation. Paclitaxel loaded CCPM had a size of 70-150 nm (depending on the PTX content), and the acid-labile acetal groups on the block copolymer rendered the CCPM pH-sensitive, leading to their rapid hydrolysis and disintegration at acidic pH, which also resulted in increased release of encapsulated PTX. The PTX-containing CCPM demonstrated increased anti-tumor activity in vitro when incubated with RAW 264.7 cancer cells. In a subsequent study [96], the same group combined the above described block copolymer with a galactose-PEG-*b*-poly( $\epsilon$ -caprolactone) (Gal-PEG-*b*-PCL) copolymer to obtain  $\beta$ -D-galactose modified PM by co-self-assembly of the two block copolymers, and core-crosslinked them using the same method as described above. Galactosamine, which binds to the asialoglycoprotein receptor (which is present on hepatocytes) was used for active targeting to hepatocellular carcinoma. The galactosamine-modified CCPM had a size of 92-136 nm and again demonstrated increased PTX release in acidic conditions. In *in vivo* biodistribution studies in mice bearing SMMC-7721 hepatoma tumors, enhanced tumor accumulation and improved antitumor efficacy was reported [96].

Convincing evidence for an improvement in the biodistribution of PM upon core-crosslinking via radical polymerization was provided by Rijcken et al., who developed ~70

nm-sized biodegradable PM based on methacrylated mPEG-b-[N-(2-hydroxyethyl)-methacrylamide]-oligolactate] (mPEG-b-pHEMAM<sub>n</sub>Lac<sub>n</sub>) block copolymers (Figure 5A) [48]. These micelles were core-crosslinked by photopolymerization of the methacrylate groups in the core-forming block (figure 5B), and demonstrated increased stability (also in the presence of SDS) while maintained their biodegradability (due to hydrolysis of the oligolactate side chains over time). As a result of core-crosslinking, a substantially improved pharmacokinetic profile was observed, with 50 % of the injected dose of CCPM still present in systemic circulation at 8 h after i.v. administration (Figure 5C). Non-crosslinked polymeric micelles (NCPM) were rapidly cleared, and were barely detectable at time points exceeding 4 h (Figure 5C). This prolonged circulation half-life time led to a substantial improvement in tumor accumulation: for CCPM, approximately 5% of the injected dose was found to be present per gram tumor at 48 h p.i., while no tumor accumulation could be detected at this time point for NCPM (Figure 5D). These findings exemplify the importance of core-crosslinking on the pharmacokinetic and biodistributional properties of PM.

### 3.2. Core-crosslinking of PM using reactive block copolymers and bi-functional agents

Bi-functional agents are used as crosslinkers for polymeric micelles when the core-forming block contains reactive functionalities (Figure 4B). A representative example for this type of core-crosslinking is the use of reactive groups that are stable during polymer synthesis, but easily addressable for additional polymer modifications [97, 98], and also lipophilic enough to not disturb micelle formation. The advantage of this type of crosslinking over radical polymerization is that in many cases the side group or end-functionality of the polymer can be directly used, without the need for previous modification.

In this respect, Siegwald et al. used block copolymers of polydiethyleneglycol methacrylates (PDEGMA) with epoxy-bearing acrylates to prepare a library of self-assembled nanoparticles with hydrophilic cores (nanohydrogels), which were subsequently core-crosslinked using diamines [50]. In the same study, also amphiphilic block copolymers were pre-assembled and core-crosslinked, to form CCPM-like nanoparticles. The library of nanoparticles was extensively characterized (physicochemically, siRNA and pDNA complexation efficiency, siRNA and DNA delivery *in vitro*, and siRNA delivery to hepatocytes *in vivo*), revealing structure-function relationships and strategies for the design of efficient formulations. Following up on this, Nuhn and colleagues used amphiphilic block copolymers based on poly(pentafluorophenol methacrylate) and tri(ethylene glycol)-methyl ether methacrylate, which upon self-assembly were core-crosslinked using amine-containing crosslinkers, and which were shown to enable efficient siRNA delivery *in vitro* [99]. In another representative approach for the use of bifunctional crosslinking agents, Leroux and coworkers used divinyl sulfone, to crosslink the cores of reversed PM based on star-shaped alkylated poly(glycerol methacrylate) using a Michael addition reaction, forming 50 nm micelles [100]. These micelles were loaded with model dyes, and presented with more sustained release kinetics as compared to their non-crosslinked counterparts.

Bronich and colleagues have made important contributions on the stabilization of block ionomer complex (BIC) micelles via bifunctional agents, to overcome issues related to instability of the ionic core in the presence of charged blood components (recently reviewed

in [103]). In their work, BIC micelles based on block copolymers of poly(ethylene glycol)-*b*-poly(methacrylic acid) (PEG-*b*-PMA) combined with divalent metal ions were crosslinked via the reaction of the carboxylic groups of PMA with 1,2-ethylenediamine, followed by removal of the cations (Figure 6A), resulting in ~170 nm core-crosslinked BIC micelles [104]. Since polymethacrylic and polyacrylic acid are insoluble in water in the presence of elevated calcium ion concentrations [105], the resulting self-assemblies have hydrophobic cores and are considered micellar structures. In follow-up studies, DOX-loaded CCPM were prepared, which were stable for a prolonged period of time, and demonstrated an accelerated DOX release at acidic pH due to the protonation and swelling of the micellar core [106]. The *in vitro* release of DOX from the CCPM at physiological conditions was not only more sustained, but also more complete than the release from two clinically relevant formulations, i.e. Doxil (liposomal DOX) and SP1049C (DOX in Pluronic micelles). In a cell viability experiment, the DOX-loaded CCPM demonstrated increased cytotoxicity as compared to DOXIL when incubated with A2780 cells, but less than SP1049C and free DOX. Similar core-crosslinked BIC micelles were loaded with the highly hydrophilic alkylating agent cisplatin, confirming sustained release profiles at physiological conditions also for this chemotherapeutic agent (Figure 6B) [101]. The cisplatin-loaded micelles were effectively taken up by A2780 cells, and cisplatin was found to be localized in vesicular compartments within the cells. Upon i.v. injection into mice bearing A2780 ovarian carcinoma xenografts, a longer circulation time and an increased tumor accumulation of cisplatin was observed when loaded in CCPM (as compared to the free drug; Figure 6C-D) [102]. The CCPM also displayed a better safety profile than free cisplatin: the latter caused significant weight loss, increased serum BUN (blood urea nitrogen) levels and renal tubular toxicity, while the CCPM caused none of these side effects. Extending these efforts even further, Bronich et al. actively targeted their cisplatin-containing CCPM to cancer cells, by introducing folate on the surface of the micelles [107]. This resulted in enhanced cellular uptake, and in significantly increased cytotoxicity. Injection of folate-targeted CCPM into tumor-bearing mice resulted in an increased amount of cisplatin accumulating in tumors (as compared to untargeted micelles and to the free drug), as well as in superior antitumor efficacy (see section 4).

Polymerizable bi-functional crosslinking agents have also been used to core-crosslink polymeric micelles. Chan and colleagues, for instance, reported on the preparation of PM based on RAFT-synthesized poly(hydroxyethyl acrylate)-*b*-poly(*n*-butyl acrylate) (PHEA-*b*-PBA) polymers, which were crosslinked by co-polymerization of the living RAFT end groups of the PBA block and a divinyl acid-labile crosslinker [108]. The 45-80 nm-sized micelles demonstrated enhanced DOX release at pH 5 compared to pH 7.4, attributed to the cleavage of the acetal crosslinker in acidic environment. Huang and coworkers developed dopamine-containing poly(ethylene glycol)-*b*-poly(2-methyl-2-carboxyl-propylene-carbonate)-*b*-poly(L-lactide) (mPEG-*b*-PMCC-*b*-PLA) triblock copolymers to form PM, and core-crosslinked them via oxidative self-polymerization of dopamine in the presence of oxygen. The resulting ~115 nm-sized CCPM were loaded with DOX, and their cellular uptake was shown to be significantly more efficient than that of NCPM (which was attributed to their smaller size and greater stability) [109].

### 3.3. Core-crosslinking by disulfide bridge formation

Disulfide bridges are often used for core-crosslinking of polymeric micelles, mainly because of their *in vivo* reversibility. The reduction potential in the blood stream is known to be weak (glutathione levels in the range of 2-20  $\mu\text{M}$ , [110]) and thus cannot cleave disulfide bonds. However the intracellular area is much more reducing (glutathione levels 0.5-10 mM [110]), and especially in antigen-presenting cells, these elevated levels are reached already within the endosomal compartments [111, 112]. Thus, disulfides can provide stability in the systemic circulation, but are rapidly cleaved in reductive intracellular environments [110]. In many cases, disulfide crosslinks are introduced in the micellar core, via bi- or multi-functional agents containing disulfide bridges. For example, Bronich et al. modified the core of block ionomer complexes (BIC) based on poly(ethylene oxide)-*b*-poly(methacrylic acid) (PEO-*b*-PMA) and divalent metal cations ( $\text{Ca}^{2+}$ ) with cystamine, rendering  $\sim 100$  nm-sized BIC micelles with biodegradable disulfide crosslinks which disintegrated in the presence of DTT [113]. DOX was loaded into these micelles, and an accelerated release was observed in the presence of glutathione and cysteine. Cheng et al. prepared  $\sim 50$  nm-sized micellar nanocarriers using block copolymers containing alkyne side chains and crosslinked them via bis-azidoethyl disulfide by means of click chemistry [114]. These CCPM demonstrated improved stability compared to NCPM, as well as controlled release of encapsulated dyes in response to reducing agents. Zhong and colleagues used a catalytic amount of dithiothreitol (DTT) to core-crosslink PM based on poly(ethylene glycol)-*b*-poly(*N*-2-hydroxypropyl methacrylamide)-lipoic acid (PEG-*b*-pHPMA-LA), obtaining  $\sim 100$  nm-sized CCPM which could be loaded with DOX [115]. Enhanced drug release was observed upon exposure to reducing conditions (87%, upon 12 h in the presence of DTT) as compared to physiological conditions (23%; upon 12 h in PBS). It has to be kept in mind, however, that DDT is not a biologically very relevant reducing agent, as it has a much higher reducing potential than glutathione. Glutathione should therefore also be considered when studying the intracellular behaviour of these systems, as it is endogenously present in high concentrations in the cytoplasm of cells. The same group also developed PM based on lipoic acid and *cis*-1,2-cyclohexane-dicarboxylic acid (CCA) modified poly(ethylene glycol)-*b*-poly(L-lysine) (PEG-P(LL-CCA/LA)) block copolymers, and crosslinked them with a catalytic amount of DTT [116]. The CCPM showed enhanced stability in high dilutions and in the presence of salts, but rapidly dissociated upon addition of DTT. DOX loaded CCPM showed slow release at physiological pH, which was however accelerated (doubled) when placed at pH 5 (endosomal pH), possibly due to the degradation of the acid-sensitive bonds of CCA. In addition, a rapid DOX release was demonstrated in the presence of glutathione (more than 85 % in 24 hours), showing that this system is sensitive to both pH and reduction. Finally, the DOX loaded CCPM demonstrated increased cytotoxicity against HeLa and HepG2 cells.

Disulfide core-crosslinking has also been performed using polymers containing free thiols, and in that case crosslinking takes place under oxidative conditions. Kataoka and colleagues for instance introduced iminothiolane groups into block copolymers based on poly(ethylene glycol)-*b*-poly(L-lysine) (PEG-*b*-PLL-IM), and prepared disulphide-crosslinked polyion complex (PIC) micelles via complexation with siRNA [117]. It is important to keep in mind that the reaction of 2-aminothiolane with primary amines is not free of side reactions. Besides the uncontrolled oxidation to disulfides, the free thiol groups formed can recycle by

attacking the amidine carbon. This can then rearrange into an iminothiolane, which eventually ties up the thiol [118] and leads to hydrophobic groups within the polymer. The resulting ~60 nm-sized PIC micelles remained stable under physiological conditions, and disintegrated in a reductive environment (addition of DTT). These disulfide-core-crosslinked PIC micelles demonstrated a ~100-fold increased transfection efficiency as compared to non-crosslinked PIC micelles (as the latter are unstable at physiological ionic strength). Analogously, Mao et al. prepared thiolated poly(ethylene glycol)-b-polyphosphoramidate (PEG-b-PPA) PIC micelles containing DNA, and core-crosslinked them via the thiol groups present in the micellar core [119]. The CCPM demonstrated high stability in the presence of serum, as well as under high salt conditions, but showed efficient DNA de-complexation and release after incubation with glutathione. As a result of this, the CCPM demonstrated much higher *in vitro* DNA transfection efficiency as compared to NCPM.

Li and coworkers developed thiolated telodendrimers (i.e. linear dendritic polymers; based on linear polyethylene glycol (PEG) and a dendritic cluster of cysteine-containing cholic acids), which efficiently self-assembled into micelles and which were subsequently core-crosslinked via oxidation of the thiol groups (Figure 7A) [120]. The ~30 nm-sized micelles were loaded with paclitaxel, and a glutathione-responsive release was confirmed. Using *in vivo* optical imaging, the circulation kinetics and the biodistribution of the CCPM and the NCPM were analyzed [120]. The BODIPY 650/665 dye was conjugated to the telodendrimers themselves (to monitor the fate of the carrier), and the hydrophobic DiD dye was physically entrapped in the micellar core (to monitor the fate of a (model) drug). As shown in Figure 7B, the CCPM circulated much longer as compared to NCPM (~8-times higher BODIPY signal at 8 h post i.v. injection). In line with this, also for DiD, a 2-3-fold increase in the levels present in systemic circulation could be observed (Figure 7C). This beneficial pharmacokinetic profile resulted in inefficient EPR-mediated passive drug targeting. The *in vivo* biodistribution of DiD was evaluated *in vivo* and *ex vivo* using fluorescence reflectance imaging, and as convincingly shown in Figure 7D, the disulfide-core-crosslinked telodendrimer-based PM presented with prominent levels of tumor accumulation in mice bearing SKOV-3 ovarian carcinoma xenografts. Follow-up studies, in which DiD was replaced by chemotherapeutic drugs, were also performed. These findings are described in section 5.

### 3.4. Other types of crosslinking

Core-crosslinking of polymeric micelles has also been reported using other types of chemistries. For instance, in an interesting follow-up study of the thiolated telodendrimer-based system introduced above (see section 3.3; [120]), the same group of authors developed micelles based on these telodendrimers but this time reversibly crosslinked them via the formation of boronate esters in the micellar core [121, 122] (Figure 8A). The CCPM were ~20 nm in diameter, and stable in the presence of 50% human plasma and in SDS at physiological pH. However, when incubated with SDS at pH 5, or with SDS mixed with the competing diol mannitol, they rapidly disintegrated, due to dissociation of the boronate esters. The micelles were loaded with paclitaxel and a stimuli-responsive release was observed under the conditions mentioned above (Figure 8B). The authors also evaluated the



circulation kinetics and the biodistribution of NCPM and boronate-core-crosslinked PM. This was done using fluorescence reflectance imaging (Figure 8C) and using a FRET-based technique (Fluorescence Resonance Energy Transfer, via which the molecular proximity of a FRET acceptor-donor pair can be estimated; Figure 8D). In case of the latter, the green dye DiO was encapsulated in the micelles and acted as donor, while the red-orange dye rhodamine B was covalently linked to the micelles and acted as the acceptor. As shown in Figure 8D, in case of NCPM, the FRET-dependent signal of rhodamine B in blood rapidly disappeared, hinting toward rapid micelle disintegration and/or rapid DiO release. In the case of CCPM, the FRET signal could be detected up to 24 h, exemplifying enhanced micelle stability *in vivo* upon core-crosslinking. *Ex vivo* optical imaging of tumors and organs 32 h after the i.v. injection of DiD-loaded CCPM in SKOV-3 tumor-bearing mice finally indicated that the developed boronate ester-core-crosslinked polymeric micelles accumulated in tumors effectively and selectively via EPR (Figure 8C).

Core-crosslinking of polymeric micelles has also been reported using functional groups inducing dimerization upon UV exposure, such as cinnamic acid, coumarin and thymine. Kim and colleagues, for instance, introduced photo-crosslinkable cinnamate groups on poly(aspartamide) derivatives containing mPEG and imidazole [123]. The resulting polymers self-assembled into ~150 nm-sized PM, and were crosslinked by UV irradiation, leading to dimerization of the cinnamate groups in the micellar core. Non-crosslinked micelles displayed pH-dependent dissociation (due to the protonation of the imidazole groups in acidic environments; leading to a hydrophobic to hydrophilic transition), while CCPM retained their stability. The latter did present pH-dependent swelling-shrinking behaviour. Consequently, encapsulated paclitaxel could be released in a well-controlled manner from CCPM, while in case of NCPM, a large burst release was observed [123].

Silicon chemistry has also been employed as a method for PM core-crosslinking [42]. As an interesting example, Li and colleagues synthesized poly(PEG-methacrylate)-*b*-poly(triethoxysilyl propylmethacrylate) (PPEGMA-*b*-PESPMA) block copolymers, which formed micelles with ethoxysilane-based cores [124, 125]. A triethoxysilane-modified Cy7-like near-infrared fluorophore (NIRF) was encapsulated, and the loaded micelles were crosslinked by condensation of the ethoxysilane groups (including those of the dye), resulting in ~25 nm-sized CCPM. The results obtained in this study are described in more detail below (see section 4 and Figure 11).

#### 4. Co-crosslinked (pro-) drugs

In the previous section it is clearly demonstrated that core-crosslinking of polymeric micelles substantially improves their *in vivo* stability, circulation time and biodistribution, leading to enhanced accumulation at the target site. However, a prolonged blood circulation of CCPM does not necessarily imply that the payload to be delivered via the micelles will be retained in the micellar core. This was demonstrated in the work of Rijcken et al. in which, even though mPEG-*b*-pHEMAM<sub>n</sub>-based CCPM showed remarkable circulation kinetics (Figure 5) [48], the encapsulated paclitaxel was rapidly eliminated from the systemic circulation (Figure 9A), resulting in moderate to low levels of tumor accumulation (<2% ID/g; Figure 9B) [126]. Consequently, it is evident that the drug has to be covalently (and



reversibly) linked to the micellar core, to ensure its retention within the micelles during the circulation, and to enable release in a controlled and sustained manner upon reaching the target site. To that end, using a similar micellar platform (based on mPEG-b-pHPMAmLac<sub>n</sub> block copolymers) and dexamethasone as a prototypic anti-inflammatory agent, a methacrylated version of dexamethasone containing a degradable carbonate ester was prepared, and this was co-crosslinked within the micellar core. Co-crosslinking of the methacrylated prodrug was possible by co-polymerization of the methacrylate groups of the prodrug with the methacrylate groups present on the polymeric blocks forming the micellar core (Figure 10A). As shown in Figure 9C, upon covalent drug entrapment, the active agent seemed to follow the fate of the micelles, and remained in the circulation for a prolonged period of time, resulting in significantly enhanced tumour accumulation (up to 10% of the injected dose per gram tissue; Figure 9D) [41]. In the case of the free drug or DEX physically encapsulated (i.e. non-covalently) in mPEG-b-pHPMAmLac<sub>n</sub> micelles, rapid clearance from the systemic circulation was observed (Figure 9C). These findings convincingly show that covalent drug attachment in the core of CCPM results in an improved pharmacokinetic and biodistributional profile, with the majority of the drug remaining associated with the micellar nanocarrier up until 48 h after i.v. administration. Consequently, it seems as if covalent drug attachment, in addition to core-crosslinking, is necessary to achieve efficient micelle-mediated passive drug targeting.

In a follow-up study of the CCPM micelles with covalently entrapped DEX described above, Crieleard and colleagues used three different methacrylated DEX derivatives that contained linkers with different hydrolysis rates, to tailor the drug release kinetics [127]. The DEX derivatives used contained a methacrylated group linked to DEX via a sulphide, sulfoxide, or sulfone ester linker (Figure 10B). These thioethers have different degrees of oxidation, which were expected to change the hydrolysis kinetics of the neighboring ester group, thereby tailoring the drug release kinetics. After physical encapsulation of these derivatives in the PM, the system was co-crosslinked by co-polymerization of the methacrylate groups of the prodrug and of the polymer (Figure 10A). This resulted in efficiently loaded CCPM with an average diameter of 70 nm. Next, the release kinetics of DEX from the micelles were compared for the three DEX prodrugs. The PM with sulfide ester linked DEX demonstrated the slowest release kinetics (<5% in 7 days), which was faster in the case of sulfoxide linked DEX, while the fastest release was observed by the sulfone ester linked DEX (Figure 10B). The CCPM with the most accelerated release kinetics (sulfone ester linked DEX), were then tested *in vivo* against arthritis (see section 5).

Using the same mPEG-b-pHPMAmLac<sub>n</sub>-based micellar platform, Talelli and co-workers co-crosslinked a methacrylated doxorubicin derivative containing an acid-labile hydrazone linker in the core of CCPM (Figure 10C) [49]. The micelles demonstrated very low drug release at pH 7.4 (less than 10% in 24 h), but release was almost quantitative upon 24 h of incubation at pH 5 (Figure 10C). This indicates that upon covalent attachment, the drug will stay in the CCPM while in circulation, but can be released upon accumulation in the slightly acidic extracellular environment in tumors, as well as upon cellular uptake in the acidic lysosomes of cancer cells. In a follow up study the micelles were also actively targeted by conjugating an anti-EGFR nanobody on their surface, which led to enhanced cellular uptake,

while no differences in release kinetics and size characteristics were noted [128]. Both the passively and the actively targeted mPEG-b-pHPMAmLac<sub>n</sub>-based CCPM were also evaluated *in vivo*, in mice bearing B16F10 melanoma or 14C tumors. These results are described below, in Section 5 (Preclinical efficacy of CCPM).

In the work of Li and colleagues briefly described in section 3.4, silicon chemistry was used to core-crosslink PM and to covalently attach a dye in the crosslinked core, using micelles with ethoxysilane groups in their cores based on poly(PEG-methacrylate)-*b*-poly(triethoxysilyl propylmethacrylate) (PPEGMA-*b*-PESPMA) block copolymers [125]. A triethoxysilane-modified Cy7-like near-infrared fluorescence (NIRF) dye was loaded and core-crosslinking and covalent dye entrapment was performed by co-condensation of the silane groups (of the polymer and of the dye), resulting in ~ 25 nm-sized CCPM. To follow the fate of the carrier, the micelles were labelled with indium-111. Upon i.v. injection, prolonged circulation kinetics of the micelles was observed in mice, with up to 9% of the injected dose still present in the systemic circulation at 48 h post i.v. administration. The biodistribution and the target site accumulation of these ethoxysilane-core-crosslinked polymeric micelles (containing a covalently attached model drug) were analyzed upon i.v. injection into mice bearing MDA-MB-468 breast cancer xenografts [125]. Non-invasive imaging of the mice demonstrated a significant tumor accumulation of both the micelles (visualized by gamma-scintigraphy of the <sup>111</sup>In label of the micelles) and the NIRF dye (NIRF optical imaging) 120 hours post injection, demonstrating that by co-crosslinking of the cargo in the PM core, it follows the fate of the CCPM and the premature diffusion/release is avoided. However, in this study, the dye was non-reversibly linked in the micellar core, therefore making this system mainly suitable for tumor imaging, but not for drug delivery purposes, where a controlled release is necessary. Therefore in a follow-up study, the same group of authors developed a similar type of micelles, but on this occasion, the pendant triethoxysilanes were linked on the polymer via a degradable succinic ester linker (which degrades in acidic environments), to make the crosslinking reversible, and to thereby add to the system controlled release properties [124]. The NIR fluorophore 3-triethoxysilyl-propyl IR783 was used as a model drug, and loaded into the ~25 nm-sized micelles (Figure 11A). In order to follow the fate of the micelles, these were radiolabelled with <sup>111</sup>In. The reversibly core-crosslinked micelles demonstrated a prolonged circulation time upon injection to healthy mice (Figure 11B), and upon injection to CT-26 tumor bearing mice, up to 8% of the injected dose of radioactivity was detected tumors (Figure 11C). Finally, *in vivo* optical imaging was employed to show that the covalently entrapped model drug IR783 efficiently accumulated in CT-26 tumors, and was efficiently retained there over time (Figure 11D). These well-performed studies and promising findings call for follow-up experiments focusing on the therapeutic efficacy of these formulations.

Using the boronate ester chemistry described in Section 3.4, Kataoka and coworkers covalently entrapped siRNA in the core of CCPM [10]. To this end, part of the lysine groups of PEG-b-PLys block copolymers was modified with 3-fluoro-4-carboxy phenylboronic acid. Phenylboronic acid is known to form reversible esters with the diols present on the ribose ring at the 3'-end of RNA, and the block copolymers synthesized were consequently able to chemically retain siRNA in the micellar core. The developed systems disassembled

upon addition of the ribose competitor adenosine triphosphate (ATP; used at physiologically (intracellularly) relevant concentrations), leading to siRNA release. This exemplified the ribose-specific stabilization of the complexes, as well as the specific intracellular ATP-dependent release of siRNA.

As another example, Cheng and colleagues used alkyne-containing block copolymers to form PM, which were then core-crosslinked by clicking the alkyne groups in the core with the reduction-sensitive bis-azide crosslinker bis(azidoethyl)-disulfide, to result in CCPM that can disintegrate intracellularly. A disulfide containing camptothecin prodrug was covalently linked in the micellar core and reduction-dependent drug release and cytotoxicity was demonstrated [129]. Bulmus et al. conjugated hydrazone-maleimide-modified DOX to part of the thiol-containing hydrophobic blocks in PEG-poly(pyridyldithioethyl methacrylate) micelles, while the remaining part of the thiol groups was used to form crosslinks in the core [130]. Due to the linkage of the drug through a hydrazone spacer, the micelles displayed pH-dependent release, which was shown to accelerate at acidic conditions. Cisplatin has also been covalently attached in the core of CCPM, using isocyanate-modified block copolymers and crosslinking via reaction of the isocyanate groups of the polymer with the amine groups of a Pt(IV)-prodrug, which was prepared from the parent compound cisplatin [131]. The resulting CCPM were ~35 nm in diameter and released 82% of the cargo in 22 days.

Other than the selected examples briefly described above, there are many other studies focused on polymer drug conjugates (usually with a stimuli-responsive linker) that self-assembled into micelles [31, 53, 63, 64, 105]. However, these systems are not crosslinked and simply rely on the assembly of the classical polymer-drug conjugates into PM, and therefore fall out of the scope of this review which is focused on core-crosslinked polymeric micelles. For further reading on this type of micelles, the reader is referred to two recent reviews [34, 62].

## 5. Preclinical efficacy of core-crosslinked polymeric micelles

Although there are a lot of interesting and innovative chemistries published in the literature on the preparation of CCPM, there is only a relatively small number of publications that provide proof-of-principle for an improved *in vivo* therapeutic efficacy of CCPM. In a few of the studies mentioned above, *in vivo* efficacy analyses were also performed, which will be described separately in this section. For instance, the micelles based on the cysteine-modified telodendrimers composed of linear PEG and a dendritic cluster of cholic acids crosslinked via disulfide bridges (see section 3.3 and Figure 7) were also studied with regard to efficacy [120]. In these experiments, it was found that paclitaxel-loaded CCPM were significantly more effective than both free PTX and PTX entrapped in non-crosslinked micelles (Figure 12A). The cisplatin-loaded BIC micelles developed by Bronich and colleagues (see section 3.2 and Figure 6) were also tested for antitumor efficacy *in vivo*, upon injection into female nude mice bearing A2780 tumor xenografts [102]. As shown in Figure 12B, the tumors of mice treated with CCPM demonstrated significantly decreased tumor growth (and also significantly increased survival) as compared to free cisplatin. At the same time, treatment with cisplatin-loaded CCPM did not result in weight loss, as opposed

to treatment with free cisplatin. When the same BIC micelles were also actively targeted, via the incorporation of folate moieties on their surface, tumour growth inhibition could be even further enhanced in mice bearing A2780 xenografts (Figure 13A) [107].

Similarly, as detailed in Chapter 4 and Figure 9, when paclitaxel was entrapped in non-core-crosslinked mPEG-*b*-pHPMAm-Lac<sub>n</sub>-based polymeric micelles, a very low tumor accumulation was observed in mice bearing 14C xenografts [126]. As expected, this did not result in a therapeutic benefit, with PTX-loaded NCPM presenting with the same antitumor efficacy as free paclitaxel [132], most likely because of both micelle instability in systemic circulation and premature release of PTX from the micelles. However, when the mPEG-*b*-pHPMAm-Lac<sub>n</sub>-based micelles were core-crosslinked, and when a methacrylated version of dexamethasone was covalently entrapped in the micellar core, the therapeutic efficacy could be improved as compared to the free drug: as a result of the much longer circulation time and the efficient tumor accumulation of the dexamethasone-containing CCPM (Figure 8C-D), the growth B16F10 tumors could be inhibited more efficiently than upon treatment with free dexamethasone (Figure 12C) [133]. In this specific case, dexamethasone was linked to the core of the CCPM through a sulfide linker, which demonstrated rather slow release kinetics. As a consequence, when compared to dexamethasone-loaded liposomes (which rapidly release their payload upon phagocytosis by tumor-associated macrophages), growth inhibition was somewhat less prominent in the rapidly growing B16F10 tumor model. More rapidly releasing linkers therefore seem to be necessary for efficient disease treatment in such aggressively growing mouse models.

In the case of doxorubicin, Talelli et al. therefore employed a hydrazone linker to attach the drug to the micellar core. As detailed above (see Chapter 4), hydrazone linkers slowly release DOX at pH 7.4, while completely release their payload within 24 h at pH 5. CCPM based on mPEG-*b*-pHPMAm-Lac<sub>n</sub> with covalently attached doxorubicin were evaluated *in vivo* in mice bearing B16F10 tumors, and were shown to be significantly more effective in inhibiting tumor growth (and prolonging survival) than was free doxorubicin (Figure 12D) [49]. The same micelle formulation was also actively targeted, using an anti-EGFR nanobody (EGa1). In this case, the aim of active targeting was not to improve the overall tumor accumulation of the CCPM, but to facilitate their cellular uptake [128] and to enhance their antitumor efficacy (as EGa1 nanobodies possess intrinsic tumor growth inhibiting properties). As shown in Figure 13B, when evaluated *in vivo* in mice bearing UM-SCC-14C head and neck squamous carcinomatumors, EGa1 nanobody-targeted CCPM containing covalently attached doxorubicin presented with superior antitumor efficacy as compared to all relevant control regimens. Interestingly, as hypothesized, also drug-free nanobody-targeted micelles showed reasonable tumor growth inhibition, to an extent similar to that obtained for free doxorubicin (administered at its maximum tolerated dose (MTD); 5 × 3 mg/kg). Due to the absence of toxicity for DOX-containing mPEG-*b*-pHPMAm-Lac<sub>n</sub> micelles at doses equivalent to the MTD of free DOX, both the passively and the actively targeted CCPM were also evaluated at higher doses (4 × 9 mg/kg DOX-equivalent). Both high-dose treatments were more effective than the lower dose CCPM treatment, and there was a tendency toward more efficient therapy using high-dose nanobody-targeted interventions, with significant differences in tumor growth inhibition at several time points

during follow-up (Figure 13B), and with a clearly prolonged survival of animals treated with nanobody-modified CCPM [134].

Also in non-cancerous disorders, such as rheumatoid arthritis, CCPM containing covalently attached drugs have been shown to outperform free drugs and/or CCPM with physically entrapped drugs. A representative example of this has been published by Crielaard et al, who developed three different thioether linkers for controlled glucocorticoid release from CCPM, and who tested the most rapidly releasing formulation in mice and rats suffering from collagen-antibody induced arthritis and adjuvant-induced arthritis [127]. Mice treated with DEX-containing CCPM showed a strong and long-lasting reduction of arthritis symptoms as compared to the free drug (Figure 14A-B). Upon a single-dose treatment with micelles at DEX-equivalent doses of 5 and 10 mg/kg, disease activity could be repressed almost to the level of healthy mice. Similar results were obtained in rats [127].

In a follow-up first-of-its-kind head-to-head comparison study, the *in vivo* efficacy of CCPM containing covalently attached DEX was compared to that of three other nanomedicine formulations (i.e. liposomal DEX, a rapidly releasing pHPMA-DEX polymer conjugate, and slowly releasing pHPMA-DEX polymer conjugate), as well as to free DEX, in an adjuvant-induced arthritis rat model [135]. As shown in Figures 14C-D, it was found that the best performing formulations were DEX-containing CCPM and the slowly releasing pHPMA-DEX polymer conjugate, which both efficiently suppressed disease symptoms for up to 4 weeks after a single injection. This comparative analysis convincingly shows that CCPM are among the best performing nanomedicine formulations, at least in this particular disease model. Similar studies in other disease models, e.g. in tumor-bearing mice, are eagerly awaited, not only to evaluate the most optimal nanomedicine formulation for treating a specific disease, but also for obtaining valuable information on fundamental differences (e.g. regarding biodistribution, therapeutic efficacy, tolerability, etc) between different drug delivery systems [136].

## 6. Clinical translation of core-crosslinked polymeric micelles

Upon providing preclinical proof-of-concept for the efficacy and safety of a novel nanomedicinal product, the next step in its translation are clinical trials [137]. However, multiple criteria need to be met before entering-in-human studies (Figure 15) [15, 138]. The common goal of using nanomedicine formulations, including CCPM, is to modify the biodistributional profile of an active pharmaceutical ingredient (API) in such a way that an improved therapeutic index is obtained (as compared to the parental free API). Accordingly, a nanomedicinal product is considered a new chemical entity (NCE; US nomenclature) or a new active substance (NAS; EU nomenclature), even if it contains an approved and clinically extensively used drug. Relevant development criteria are described in a number of ICH guidelines (International Conference on Harmonisation of Technical Requirements for Registration of Pharmaceuticals for Human Use), as well as in a recent guideline of the European Medicines Agency focusing specifically on block copolymer micelles (EMA/CHMP/13099/2013; Reflection paper on the development of block copolymer micelle medicinal products). According to these guidelines, the preclinical to clinical development process comprises the study of:

- Therapeutic profile, including pharmacokinetics (PK); to prove activity.
- Safety and tolerability, including toxicokinetics (TK); to prove biocompatibility.
- Chemistry, manufacturing and control (CMC); to prove production robustness.

Below, we describe these three steps critical for the clinical translation of nanomedicines (and more specifically of (CC)PM) in more detail.

### 6.1. Therapeutic profile

Preclinical proof of efficacy and data on pharmacokinetics (PK) should be obtained in various animal models. In oncology, this refers to studies in tumor-bearing rodents, in which tumors are either subcutaneously or orthotopically inoculated, or are the result of spontaneous tumor growth in case of genetically modified animals. The guidelines for proof of efficacy are rather unspecific, except from preliminary characterisation of the mechanism of action, which is already available in case a known API is used in a nanomedicine product.

In view of systemic exposure and biodistribution profile, the EMA (European Medicines Agency) as well as the FDA (U.S. Food and Drug Administration) have provided clear guidelines for bioanalytical method development and validation (see EMEA/CHMP/EWP/192217/2009; [135]). Besides therapeutic response, it is requested to report the systemic exposure to thenano-drug in preclinical animal models, and preferably, also to the free/active API. The latter is - in our opinion - the most valid PK parameter for determining the potential of a novel drug delivery system, but unfortunately, quantitative data on local tumor exposure are hardly ever published. Consequently, an actual improvement as compared to the free API is often difficult to demonstrate, and a correlation between local free API levels and the obtained therapeutic responses is generally lacking.

Moreover, a meaningful comparison between the nanomedicine formulations currently in clinical development (which would be very useful for benchmarking-purposes; as many of these formulations contain the same API, e.g. doxorubicin, paclitaxel or irinotecan) is not possible. This is due to the large variability in the nature of these studies, related e.g. to differences in dosing regimens, tumor models, end-points and evaluation protocols. Direct head-to-head comparisons, evaluating the therapeutic efficacy of several different (PM-based) nanomedicine formulations, are therefore strongly encouraged [135].

### 6.2. Safety and tolerability

Besides PK and proof of efficacy, the safety and tolerability of a novel (PM-based) nanomedicine formulation have to be demonstrated before it can be translated into the clinic. This is generally done via several *in vitro* and *in vivo* studies, which besides feedback on overall biocompatibility often also provide useful information on the starting dose for the first clinical evaluation. Several guidelines are available for the safety assessment of novel (nano-) oncology products, such as the ICH guideline S9, on the nonclinical evaluation of anticancer pharmaceuticals (EMA/CHMP/ICH/646107/2008). Importantly, the majority of these studies have to be performed under Good Laboratory Practice (GLP). The preclinical safety package to be provided to the responsible regulatory authorities generally comprises the evaluation of the new nanomedicine formulation in at least two different



animal models (i.e. rodents and non-rodents). Depending on the type of API that is used, on pre-existing knowledge on its mechanism of action and tolerability, and on the specific composition of the formulation in question, this package may - upon discussion with the responsible regulatory authorities - be narrowed. For example, in the case of docetaxel, there is extensive knowledge available on the preclinical development of Taxotere<sup>®</sup> (see e.g. [139]), which can be used in drafting the preclinical development plan of a novel PM product containing docetaxel.

The main experiments to be performed for the preclinical safety package aim to assess toxicity upon both acute and longer-term exposure (e.g. upon 5-day repeated dosing). In these studies, the focus is on potential side effects at the whole-organism level, related e.g. to overall behaviour, food consumption, body and organ weight, and piloerection, followed by a histopathological and clinical chemical evaluation. Next, the systemic exposure to the API entrapped in the nanomedicine product, and ideally also to the free API, is determined. This is generally referred to as toxicokinetics (TK), as it allows for the correlation between time and dose of exposure, and adverse events. Accumulation in potentially endangered healthy organs should also be assessed, to exemplify that the newly developed nanomedicinal product (e.g. CCPM) improves the deleterious biodistributional profile of the original API.

Although not officially obliged by the abovementioned guidelines and the responsible regulatory authorities, it is highly advisable to also take along the empty (PM-based) nanocarrier material in such safety and tolerability analyses. Especially in the case of a completely new nanomaterial or (CC)PM composition, such analyses may facilitate the allocation of specific side effects to either the drug, or to the carrier material.

### 6.3. Manufacturing robustness

Initial preclinical studies on a new nanomedicine product (and (CC)PM) are generally performed with materials that are only characterized to a limited extent, and whose manufacturing has only been performed at laboratory scale dimensions. When aiming for clinical translation, a multiple-fold upscaling of the production of the formulations is necessary, as well as a thorough characterisation, including impurity profiling. As such, a novel (CC)PM formulation is not different from a 'traditional' NCE, and has to comply with all existing international guidelines regarding chemistry, manufacturing and control (CMC). The most important aspects that have to be addressed in this regard are:

- Are the polymeric building blocks available as GMP-grade material, with a sufficiently high purity? If not: is their synthesis upscalable with reproducible outcome?
- Is the manufacturing of the (CC)PM upscalable with reproducible outcome, regarding e.g. particle size, polydispersity, drug loading and drug release?
- How much drug is covalently and/or non-covalently entrapped within the (CC)PM? What percentage of the drug is released over time, and is it released in its native form?

- In case of CCPM: is the drug affected by the core-crosslinking process, and are there any unexpected impurities and/or drug-derivatives generated during core-crosslinking?

For the characterization of (CC)PM and other nanomedicine formulations, various analytical methods are available. However, there is no consensus yet as to which is the most correct or most optimal method (or combination of methods) to be used. This is probably due to the wide variability in the different nanoparticulate systems that have been designed and evaluated over the years. Therefore, no 'one-size-fits-all' approach is available. A recent initiative from the Nanotechnology Characterization Laboratory (NCL), established by the National Cancer Institute (NCI), allows for the evaluation of nanomedicinal products from various parties, aiming to facilitate the translation and regulatory review of nanomedicines for clinical trials. This analysis includes the assessment of their physicochemical characteristics, their in vitro properties, and their in vivo biocompatibility and efficacy, and it is ideally performed in at least two different animal models [140].

#### 6.4. Core-crosslinked polymeric micelles in clinical trials

Even though the PM products brought into clinical development in the past few decades have met great preclinical success in terms of improved therapeutic efficacy and decreased toxicity, they have only shown moderate improvement in patients in terms of pharmacokinetics, efficacy and tolerability, in particular when taking the theoretical potential that PM in principle bear into account [85, 141]. When critically reflecting on the products and progress available, the former generation of PM have mainly been solubilisers of hydrophobic API, instead of being real tumor-targeted drug delivery systems.

Upon i.v. injection, as discussed in the above sections, these nanocarriers have a high tendency for premature disintegration and/or premature drug release. Thus, only the administration and the initial blood concentrations are enhanced, while the PK profile of the native API remains largely unchanged, because the API is prematurely released, and therefore is again distributed freely throughout the body, resulting in a relatively large volume of distribution ( $V_d$ ).

On the contrary, second-generation core-crosslinked PM-based nanomedicine formulations with the API covalently entrapped in the micellar core aim to achieve a reduced accumulation in off-target tissues and a preferred accumulation in tumorous tissues via both a reduced  $V_d$  and via an improved PK profile (resulting in efficient EPR-mediated drug targeting to tumors). Currently, the disadvantage of using non-core-crosslinked PM with non-covalently entrapped API has become clear, as exemplified on several occasions throughout this review. To overcome this shortcoming, several PM products are being developed in which the drug is covalently attached in the micellar core. As exemplified by Table 1, these e.g. include NK012, consisting of PEG-PGlu covalently linked to SN-38, and NK911 comprising PEG-pAsp linked to DOX. These formulations, however, do not allow for well-controlled drug release kinetics. As explained in Section 4, controlled and stimuli-responsive drug release are highly beneficial, and there indeed is a new product, i.e. NC-6300, which consists of epirubicin linked to the core of PEG-pAsp micelles through a pH-labile linker, which has recently entered phase I clinical studies [81, 82]. Along the same

line of thinking, we foresee a bright clinical future for CCPM with covalently entrapped drug molecules, e.g. via thioether-based linkers, as such formulations assure both micelle stability in systemic circulation, and controlled drug release upon accumulation at the target site [127].

## 7. Conclusions

Over the past few decades, polymeric micelles (PM) have shown great potential for enhancing the solubility and the therapeutic potential of hydrophobic drugs. Several PM formulations have entered clinical trials, and one of them has already been approved. However, due to their dynamic nature, first generation PM still face the problem of premature disintegration in systemic circulation, and they consequently oftendo not display a real improvement in biodistribution and therapeutic efficacy vs. the parental free API.

Recent advances in polymer chemistry, bio-macromolecular engineering and nanotechnology haveenabled the synthesis of block copolymerswhich can be used to form more stable core-shell structures, and which contain functionalities allowing for core-crosslinking reactions to further stabilize PM. The resulting core-crosslinked polymeric micelles (CCPM) have been shown to be able to overcome several problems associated with conventional micellar formulations, as they are characterized by prolonged circulation times, by enhanced accumulation in tumors and at sites of inflammation via the EPR effect, and by increased therapeutic efficacy.

However, in many cases, regardless of the good circulation kinetics and target site accumulation of CCPM, the encapsulated therapeutic agents generally leak out before reaching the pathological site. To tackle this problem, CCPM have been developed in which the drug is covalently (but reversibly) entrapped within the micellar core, avoiding premature release in systemic circulation, and allowing for sustained and tailorable release kinetics upon accumulation at the pathological site. These two strategies, i.e. (i) core-crosslinking of PM and (ii) covalent drug attachment in PM, have clearly demonstrated improved biodistributional profiles in preclinical studies, and have lead to significantly enhanced therapeutic effects in comparison to non-stabilized PM systems.

Based on this preclinical success, a number of CCPM have recently started to enter clinical trials. For efficient clinical translation, several aspects and guidelines have to be taken into account, related to pharmacokinetics (PK) and proof of efficacy, to toxicokinetics (TK) and safety, and to chemistry, manufacturing and control (CMC). Upon properly addressing these issues, first-in-man and phase I clinical trials can be initiated, and initial proof of principle can be obtained on the potential of the formulation in question. In phase II and phase III trials, the CCPM subsequently need to demonstrate efficacyand ideally also superiority over the standard of care. The rational design, the chemical versatility, the broad biomedical applicability and the promising preclinical performance of CCPM are considered to provide a solid framework for making these formulations useful for the treatment of many different diseases.

## Acknowledgements

The authors gratefully acknowledge financial support by the European Research Council (ERC Starting Grant 309495: NeoNano), the European Union's 7<sup>th</sup> Framework Programme (COST-Action TD1004), and the German Research Foundation (DFG: LA2937/1-2; SFB1066-1). Marina Talelli is funded by the Juan de la Cierva program of the Spanish Ministry of Education (JCI-2012-13159).

## References

- [1]. Halperin A. *Macromolecules*. 1987; 20:2943–2946.
- [2]. Lammers T. *Int J Pharm*. 2013; 454:527–529. [PubMed: 23485339]
- [3]. Davis ME, Chen Z, Shin DM. *Nat Rev Drug Discov*. 2008; 7:771–782. [PubMed: 18758474]
- [4]. Sengupta S, Kulkarni A. *ACS Nano*. 2013; 7:2878–2882. [PubMed: 23607425]
- [5]. Wagner V, Dullaart A, Bock AK, Zweck A. *Nat Biotechnol*. 2006; 24:1211–1217. [PubMed: 17033654]
- [6]. Jain RK, Stylianopoulos T. *Nat Rev Clin Oncol*. 2010; 7:653–664. [PubMed: 20838415]
- [7]. Lammers T, Kiessling F, Hennink WE, Storm G. *J Control Release*. 2012; 161:175–187. [PubMed: 21945285]
- [8]. Juliano R. *Nat Rev Drug Discov*. 2013; 12:171–172. [PubMed: 23449291]
- [9]. Venditto VJ, Szoka FC. *Adv Drug Deliver Rev*. 2013; 65:80–88.
- [10]. Bertrand N, Leroux JC. *Journal of Controlled Release*. 2012; 161:152–163. [PubMed: 22001607]
- [11]. Lammers T. *Adv Drug Deliver Rev*. 2010; 62:203–230.
- [12]. Rizzo LY, Theek B, Storm G, Kiessling F, Lammers T. *Curr Opin Biotech*. 2013; 24:1159–1166. [PubMed: 23578464]
- [13]. Maeda H, Nakamura H, Fang J. *Adv Drug Deliver Rev*. 2013; 65:71–79.
- [14]. Maeda H. *J Control Release*. 2012; 164:138–144. [PubMed: 22595146]
- [15]. Duncan R, Gaspar R. *Mol Pharm*. 2011; 8:2101–2141. [PubMed: 21974749]
- [16]. Etheridge ML, Campbell SA, Erdman AG, Haynes CL, Wolf SM, McCullough J. *Nanomed-Nanotechnol*. 2013; 9:1–14.
- [17]. Florence AT. *J Control Release*. 2012; 164:115–124. [PubMed: 22484196]
- [18]. Heidel JD, Davis ME. *Pharm Res*. 2011; 28:187–199. [PubMed: 20549313]
- [19]. Schütz CA, Juillerat-Jeanneret L, Mueller H, Lynch I, Riediker M. *Nanomedicine*. 2013; 8:449–467. [PubMed: 23477336]
- [20]. Ma WW, Hidalgo M. *Clin Cancer Res*. 2013; 19:5572–5579. [PubMed: 23918602]
- [21]. Yardley DA. *J Control Release*. 2013; 170:365–372. [PubMed: 23770008]
- [22]. Gradishar WJ, Tjulandin S, Davidson N, Shaw H, Desai N, Bhar P, Hawkins M, O'Shaughnessy J. *J Clin Oncol*. 2005; 23:7794–7803. [PubMed: 16172456]
- [23]. Sparreboom A, Scripture CD, Trieu V, Williams PJ, De T, Yang A, Beals B, Figg WD, Hawkins M, Desai N. *Clin Cancer Res*. 2005; 11:4136–4143. [PubMed: 15930349]
- [24]. Gardner ER, Dahut WL, Scripture CD, Jones J, Aragon-Ching JB, Desai N, Hawkins MJ, Sparreboom A, Figg WD. *Clin Cancer Res*. 2008; 14:4200–4205. [PubMed: 18594000]
- [25]. Deng C, Jiang Y, Cheng R, Meng F, Zhong Z. *Nano Today*. 2012; 7:467–480.
- [26]. Gong J, Chen M, Zheng Y, Wang S, Wang Y. *J Control Release*. 2012; 159:312–323. [PubMed: 22285551]
- [27]. Matsumura Y, Kataoka K. *Cancer Sci*. 2009; 100:572–579. [PubMed: 19462526]
- [28]. Li W, Feng S, Guo Y. *Nanomedicine*. 2012; 7:1235–1252. [PubMed: 22931449]
- [29]. Kwon GS, Kataoka K. *Adv Drug Deliver Rev*. 2012; 64:237–245.
- [30]. Oerlemans C, Bult W, Bos M, Storm G, Nijssen JFW, Hennink WE. *Pharm Res*. 2010; 27:2569–2589. [PubMed: 20725771]
- [31]. Smart T, Lomas H, Massignani M, Flores-Merino MV, Perez LR, Battaglia G. *Nano Today*. 2008; 3:38–46.
- [32]. Cabral H, Kataoka K. *J Control Release*. 2014; 190:465–476. [PubMed: 24993430]

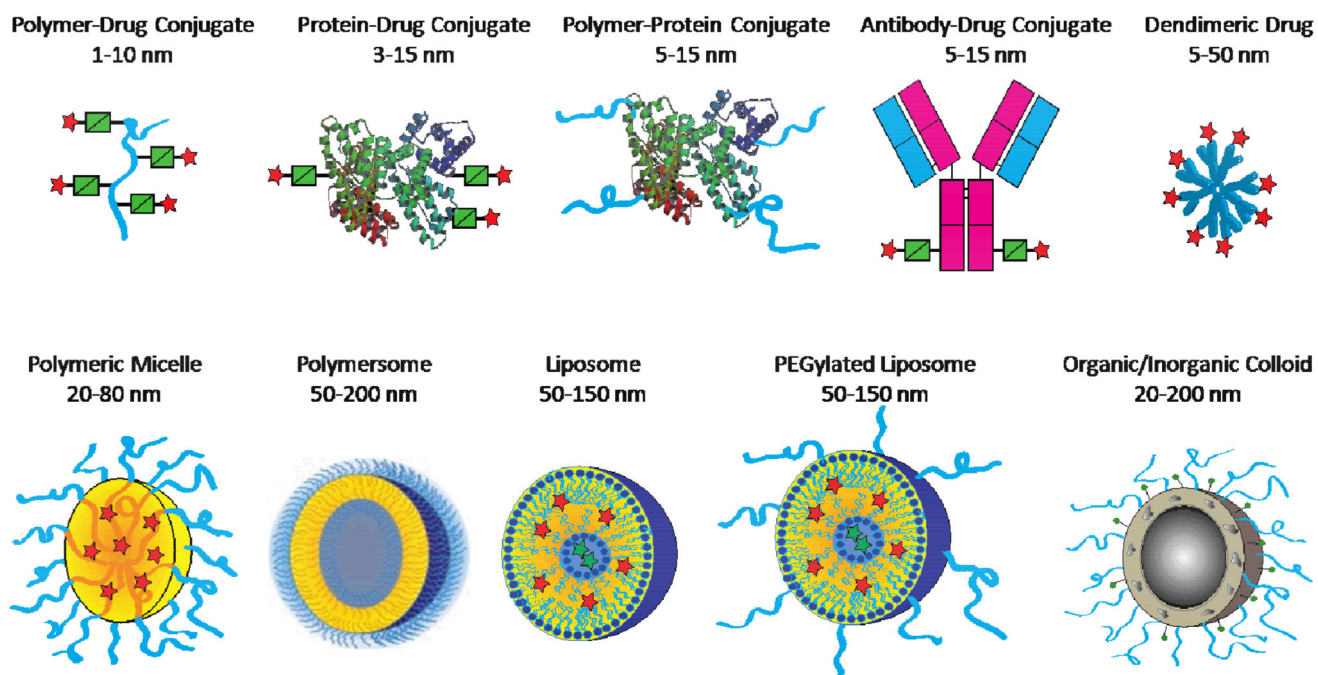
- [33]. Hennenfent KL, Govindan R. *Ann Oncol*. 2006; 17:735–749. [PubMed: 16364960]
- [34]. Rowinsky EK, Donehower RC. *New Engl J Med*. 1995; 332:1004–1014. [PubMed: 7885406]
- [35]. Torchilin VP. *Cell Mol Life Sci*. 2004; 61:2549–2559. [PubMed: 15526161]
- [36]. Kwon GS. *Crit Rev Ther Drug*. 2003; 20:357–403.
- [37]. Lu Y, Park K. *Int J Pharm*. 2013; 453:198–214. [PubMed: 22944304]
- [38]. Talelli M, Rijcken CJF, Hennink WE, Lammers T. *Curr Opin Colloid In*. 2012; 16:302–309.
- [39]. Danson S, Ferry D, Alakhov V, Margison J, Kerr D, Jowle D, Brampton M, Halbert G, Ranson M. *Brit J Cancer*. 2004; 90:2085–2091. [PubMed: 15150584]
- [40]. Hamaguchi T, Matsumura Y, Suzuki M, Shimizu K, Goda R, Nakamura I, Nakatomi I, Yokoyama M, Kataoka K, Kakizoe T. *Brit J Cancer*. 2005; 92:1240–1246. [PubMed: 15785749]
- [41]. Rijcken CJF, Talelli M, Van Nostrum CF, Storm G, Hennink WE. *Eur J Nanomed*. 2010; 3:19–24.
- [42]. van Nostrum CF. *Soft Matter*. 2011; 7:3246–3259.
- [43]. Matsumura Y, Hamaguchi T, Ura T, Muro K, Yamada Y, Shimada Y, Shirao K, Okusaka T, Ueno H, Ikeda M, Watanabe N. *Brit J Cancer*. 2004; 91:1775–1781. [PubMed: 15477860]
- [44]. Zinn T, Willner L, Lund R, Pipich V, Richter D. *Soft Matter*. 2012; 8:623–626.
- [45]. Gröschel AH, Schacher FH, Schmalz H, Borisov OV, Zhulina EB, Walther A, Müller AHE. *Nat Commun*. 2012; 3
- [46]. Gröschel AH, Walther A, Löbbling TI, Schacher FH, Schmalz H, Müller AHE. *Nature*. 2013; 503:247–251. [PubMed: 24185010]
- [47]. Moughton AO, Hillmyer MA, Lodge TP. *Macromolecules*. 2012; 45:2–19.
- [48]. Rijcken CJ, Snel CJ, Schiffelers RM, van Nostrum CF, Hennink WE. *Biomaterials*. 2007; 28:5581–5593. [PubMed: 17915312]
- [49]. Talelli M, Iman M, Varkouhi AK, Rijcken CJF, Schiffelers RM, Etrych T, Ulbrich K, van Nostrum CF, Lammers T, Storm G, Hennink WE. *Biomaterials*. 2010; 31:7797–7804. [PubMed: 20673684]
- [50]. Siegwart DJ, Whitehead KA, Nuhn L, Sahay G, Cheng H, Jiang S, Ma M, Lytton-Jean A, Vegas A, Fenton P, Levins CG, Love KT, Lee H, Cortez C, Collins SP, Li YF, Jang J, Querbes W, Zurenko C, Novobrantseva T, Langer R, Anderson DG. *P Natl Acad Sci USA*. 2011; 108:12996–13001.
- [51]. Lee JS, Feijen J. *J Control Release*. 2012; 161:473–483. [PubMed: 22020381]
- [52]. Gohy JF. *Advances in Polymer Science*. 2005:65–136.
- [53]. Mortensen K. *Curr Opin Colloid In*. 1998; 3:12–19.
- [54]. Riess G. *Prog Polym Sci*. 2003; 28:1107–1170.
- [55]. Zhulina EB, Borisov OV. *Macromolecules*. 2012; 45:4429–4440.
- [56]. Barz M, Luxenhofer R, Zentel R, Vicent MJ. *Polymer Chem*. 2011; 2:1900–1918.
- [57]. Obermeier B, Wurm F, Mangold C, Frey H. *Angewandte Chemie International Edition*. 2011; 50:7988–7997.
- [58]. Matsen MW. *Phys Rev Lett*. 2007; 99
- [59]. Choi SH, Lodge TP, Bates FS. *Phys Rev Lett*. 2010; 104
- [60]. Lu J, Choi S, Bates FS, Lodge TP. *ACS Macro Lett*. 2012; 1:982–985.
- [61]. Matyjaszewski, K. *Controlled/Living Radical Polymerization: Progress in ATRP*. American Chemical Society; Washington, D.C.: 2009.
- [62]. Moad G, Rizzardo E, Thang SH. *Polymer*. 2008; 49:1079–1131.
- [63]. Luxenhofer R, Han Y, Schulz A, Tong J, He Z, Kabanov AV, Jordan R. *Macromol Rapid Comm*. 2012; 33:1613–1631.
- [64]. Luxenhofer R, Fetsch C, Grossmann A. *J Polym Sci A1*. 2013; 51:2731–2752.
- [65]. Kabanov AV, Chekhonin VP, Alakhov VY, Batrakova EV, Lebedev AS, Melik-Nubarov NS, Arzhakov SA, Levashov AV, Morozov GV, Severin ES, Kabanov VA. *FEBS Lett*. 1989; 258:343–345. [PubMed: 2599097]
- [66]. Lu Y, Park K. *Int J Pharm*. 2012; 453:198–214. [PubMed: 22944304]

- [67]. Yokoyama M. *Expert Opin Drug Del.* 2010; 7:145–158.
- [68]. Lipinski CA. *J Pharmacol Toxicol.* 2000; 44:235–249.
- [69]. Kim DW, Kim SY, Kim HK, Kim SW, Shin SW, Kim JS, Park K, Lee MY, Heo DS. *Ann Oncol.* 2007; 18:2009–2014. [PubMed: 17785767]
- [70]. Kim TY, Kim DW, Chung JY, Shin SG, Kim SC, Heo DS, Kim NK, Bang YJ. *Clin Cancer Res.* 2004; 10:3708–3716. [PubMed: 15173077]
- [71]. Lee KS, Chung HC, Im SA, Park YH, Kim CS, Kim SB, Rha SY, Lee MY, Ro J. *Breast Cancer Res Tr.* 2008; 108:241–250.
- [72]. Lim WT, Tan EH, Toh CK, Hee SW, Leong SS, Ang PCS, Wong NS, Chowbay B. *Ann Oncol.* 2009; 21:382–388. [PubMed: 19633055]
- [73]. Hamaguchi T, Kato K, Yasui H, Morizane C, Ikeda M, Ueno H, Muro K, Yamada Y, Okusaka T, Shirao K, Shimada Y, Nakahama H, Matsumura Y. *Brit J Cancer.* 2007; 97:170–176. [PubMed: 17595665]
- [74]. Kato K, Chin K, Yoshikawa T, Yamaguchi K, Tsuji Y, Esaki T, Sakai K, Kimura M, Hamaguchi T, Shimada Y, Matsumura Y, Ikeda R. *Invest New Drug.* 2012; 30:1621–1627.
- [75]. Nakanishi T, Fukushima S, Okamoto K, Suzuki M, Matsumura Y, Yokoyama M, Okano T, Sakurai Y, Kataoka K. *J Control Release.* 2001; 74:295–302. [PubMed: 11489509]
- [76]. Hamaguchi T, Doi T, Eguchi-Nakajima T, Kato K, Yamada Y, Shimada Y, Fuse N, Ohtsu A, Matsumoto SI, Takanashi M, Matsumura Y. *Clin Cancer Res.* 2010; 16:5058–5066. [PubMed: 20943763]
- [77]. Matsumura Y. *Adv Drug Deliver Rev.* 2011; 63:184–192.
- [78]. Plummer R, Wilson RH, Calvert H, Boddy AV, Griffin M, Sludden J, Tilby MJ, Eatock M, Pearson DG, Ottley CJ, Matsumura Y, Kataoka K, Nishiya T. *Brit J Cancer.* 2011; 104:593–598. [PubMed: 21285987]
- [79]. Shimizu T, Kato Y. *Drug Deliv System.* 2009; 24:45–53.
- [80]. Cabral H, Nishiyama N, Okazaki S, Koyama H, Kataoka K. *J Control Release.* 2005; 101:223–232. [PubMed: 15588907]
- [81]. Harada M, Bohe I, Saito H, Shibata N, Tanaka R, Hayashi T, Kato Y. *Cancer Sci.* 2011; 102:192–199. [PubMed: 21040218]
- [82]. Takahashi A, Yamamoto Y, Yasunaga M, Koga Y, Kuroda JI, Takigahira M, Harada M, Saito H, Hayashi T, Kato Y, Kinoshita T, Ohkohchi N, Hyodo I, Matsumura Y. *Cancer Sci.* 2013; 104:920–925. [PubMed: 23495762]
- [83]. Valle JW, Armstrong A, Newman C, Alakhov V, Pietrzynski G, Brewer J, Campbell S, Corrie P, Rowinsky EK, Ranson M. *Invest New Drug.* 2011; 29:1029–1037.
- [84]. Hara E, Makino A, Kurihara K, Yamamoto F, Ozeki E, Kimura S. *Int Immunopharmacol.* 2012; 14:261–266. [PubMed: 22841811]
- [85]. Owen SC, Chan DPY, Shoichet MS. *Nano Today.* 2012; 7:53–65.
- [86]. O'Reilly RK, Hawker CJ, Wooley KL. *Chem Soc Rev.* 2006; 35:1068–1083. [PubMed: 17057836]
- [87]. Read ES, Armes SP. *Chem Commun.* 2007:3021–3035.
- [88]. Rolland A, O'Mullane J, Goddard P, Brookman L, Petrak K. *J Appl Polym Sci.* 1992; 44:1195–1203.
- [89]. Rosler A, Vandermeulen GWM, Klok HA. *Advanced Drug Delivery Reviews.* 2001; 53:95–108. [PubMed: 11733119]
- [90]. Iijima M, Nagasaki Y, Okada T, Kato M, Kataoka K. *Macromolecules.* 1999; 32:1140–1146.
- [91]. Lee WC, Li YC, Chu IM. *Macromol Biosci.* 2006; 6:846–854. [PubMed: 17039577]
- [92]. Shuai X, Merdan T, Schaper AK, Xi F, Kissel T. *Bioconjugate Chem.* 2004; 15:441–448.
- [93]. Hu X, Chen X, Wei J, Liu S, Jing X. *Macromol Biosci.* 2009; 9:456–463. [PubMed: 19089869]
- [94]. Chen J, Ouyang J, Kong J, Zhong W, Xing MM. *ACS Applied Materials & Interfaces.* 2013; 5:3108–3117. [PubMed: 23530535]
- [95]. Wu Y, Chen W, Meng F, Wang Z, Cheng R, Deng C, Liu H, Zhong Z. *J Control Release.* 2012; 164:338–345. [PubMed: 22800578]

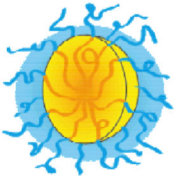
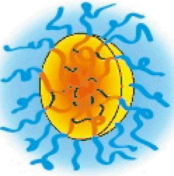
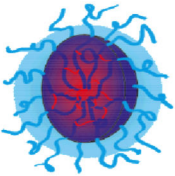
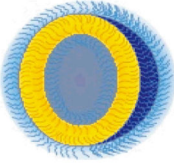


- [96]. Zou Y, Song Y, Yang W, Meng F, Liu H, Zhong Z. *J Control Release*. 2014; 193:154–161. [PubMed: 24852094]
- [97]. Gauthier MA, Gibson MI, Klok HA. *Angew Chem Int Edit*. 2009; 48:48–58.
- [98]. Theato P, Klok HA. *Functional Polymers by Post-Polymerization Modification: Concepts, Guidelines, and Applications*. 2013
- [99]. Nuhn L, Hirsch M, Krieg B, Koynov K, Fischer K, Schmidt M, Helm M, Zentel R. *ACS Nano*. 2012; 6:2198–2214. [PubMed: 22381078]
- [100]. Gao H, Jones MC, Chen J, Prud'homme RE, Leroux JC. *Chem Mater*. 2008; 20:3063–3067.
- [101]. Kim JO, Nukolova NV, Oberoi HS, Kabanov AV, Bronich TK. *Polym Sci Ser A+*. 2009; 51:708–718.
- [102]. Oberoi HS, Nukolova NV, Laquer FC, Poluektova LY, Huang J, Alnouti Y, Yokohira M, Arnold LL, Kabanov AV, Cohen SM, Bronich TK. *Int J Nanomed*. 2012; 7:2557–2571.
- [103]. Kim JO, Ramasamy T, Yong CS, Nukolov NV, Bronich TK, Kabanov AV. *Mendeleev Commun*. 2013; 23:179–186.
- [104]. Bronich TK, Keifer PA, Shlyakhtenko LS, Kabanov AV. *J Am Chem Soc*. 2005; 127:8236–8237. [PubMed: 15941228]
- [105]. Dietzsch M, Barz M, Schiöler T, Klassen S, Schreiber M, Susewind M, Loges N, Lang M, Hellmann N, Fritz M, Fischer K, Theato P, Ktöhne A, Schmidt M, Zentel R, Tremel W. *Langmuir*. 2013; 29:3080–3088. [PubMed: 23387936]
- [106]. Kim JO, Kabanov AV, Bronich TK. *J Control Release*. 2009; 138:197–204. [PubMed: 19386272]
- [107]. Nukolova NV, Oberoi HS, Cohen SM, Kabanov AV, Bronich TK. *Biomaterials*. 2011; 32:5417–5426. [PubMed: 21536326]
- [108]. Chan Y, Wong T, Byrne F, Kavallaris M, Bulmus V. *Biomacromolecules*. 2008; 9:1826–1836. [PubMed: 18564874]
- [109]. Wu S, Kuang H, Meng F, Wu Y, Li X, Jing X, Huang Y. *J Mater Chem*. 2012; 22:15348–15356.
- [110]. Meng F, Hennink WE, Zhong Z. *Biomaterials*. 2009; 30:2180–2198. [PubMed: 19200596]
- [111]. Sevier CS, Kaiser CA. *Nature Reviews Molecular Cell Biology*. 2002; 3:836–847.
- [112]. Saito G, Swanson JA, Lee KD. *Advanced Drug Delivery Reviews*. 2003; 55:199–215. [PubMed: 12564977]
- [113]. Kim JO, Sahay G, Kabanov AV, Bronich TK. *Biomacromolecules*. 2010; 11:919–926. [PubMed: 20307096]
- [114]. Zhang Z, Yin L, Tu C, Song Z, Zhang Y, Xu Y, Tong R, Zhou Q, Ren J, Cheng J. *ACS Macro Letters*. 2013; 2:40–44. [PubMed: 23536920]
- [115]. Wei R, Cheng L, Zheng M, Cheng R, Meng F, Deng C, Zhong Z. *Biomacromolecules*. 2012; 13:2429–2438. [PubMed: 22746534]
- [116]. Wu L, Zou Y, Deng C, Cheng R, Meng F, Zhong Z. *Biomaterials*. 2013; 34:5262–5272. [PubMed: 23570719]
- [117]. Matsumoto S, Christie RJ, Nishiyama N, Miyata K, Ishii A, Oba M, Koyama H, Yamasaki Y, Kataoka K. *Biomacromolecules*. 2009; 10:119–127. [PubMed: 19061333]
- [118]. Singh R, Kats L, Bittler WA, Lambert JM. *Analytical Biochemistry*. 1996; 236:114–125. [PubMed: 8619475]
- [119]. Jiang X, Zheng Y, Chen HH, Leong KW, Wang TH, Mao HQ. *Advanced Materials*. 2010; 22:2556–2560. [PubMed: 20440698]
- [120]. Li Y, Xiao K, Luo J, Xiao W, Lee JS, Gonik AM, Kato J, Dong TA, Lam KS. *Biomaterials*. 2011; 32:6633–6645. [PubMed: 21658763]
- [121]. Chen W, Cheng Y, Wang B. *Angew Chem Int Edit*. 2012; 51:5293–5295.
- [122]. Li Y, Xiao W, Xiao K, Berti L, Luo J, Tseng HP, Fung G, Lam KS. *Angew Chem Int Edit*. 2012; 51:2864–2869.
- [123]. Lin W, Kim D. *Langmuir*. 2011; 27:12090–12097. [PubMed: 21861467]
- [124]. Zhao J, Song S, Zhong M, Li C. *ACS Macro Letters*. 2012; 1:150–153. [PubMed: 22685693]

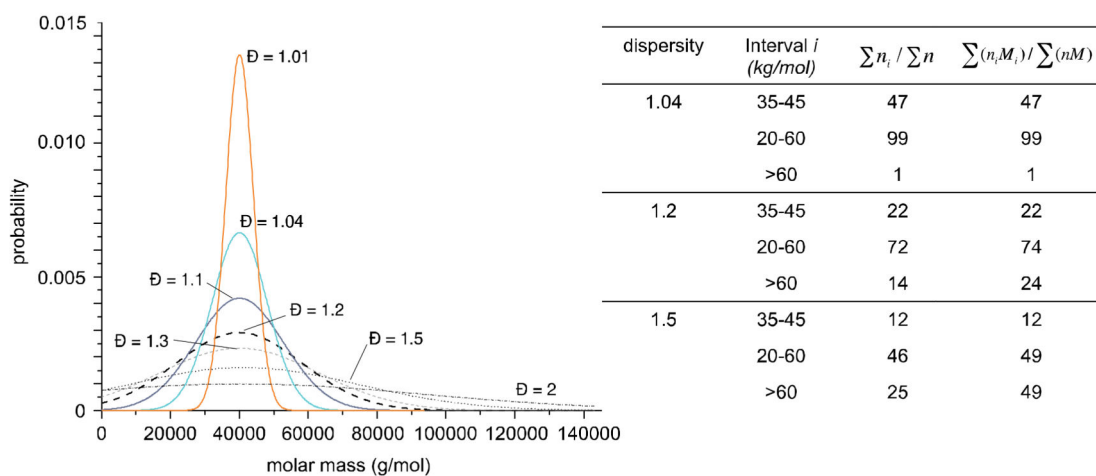
- [125]. Yang Z, Zheng S, Harrison WJ, Harder J, Wen X, Gelovani JG, Qiao A, Li C. *Biomacromolecules*. 2007; 8:3422–3428. [PubMed: 17958440]
- [126]. Rijcken, CJF. Thesis. Utrecht University; 2007.
- [127]. Crielaard BJ, Rijcken CJF, Quan L, Van Der Wal S, Altintas I, Van Der Pot M, Kruijtzter JAW, Liskamp RMJ, Schiffelers RM, Van Nostrum CF, Hennink WE, Wang D, Lammers T, Storm G. *Angew Chem Int Edit*. 2012; 51:7254–7258.
- [128]. Talelli M, Rijcken CJF, Oliveira S, van der Meel R, van Bergen en Henegouwen PMP, Lammers T, van Nostrum CF, Storm G, Hennink WE. *J Control Release*. 2011; 151:183–192. [PubMed: 21262289]
- [129]. Wang H, Tang L, Tu C, Song Z, Yin Q, Yin L, Zhang Z, Cheng J. *Biomacromolecules*. 2013; 14:3706–3712. [PubMed: 24003893]
- [130]. Jia Z, Wong L, Davis TP, Bulmus V. *Biomacromolecules*. 2008; 9:3106–3113. [PubMed: 18844406]
- [131]. Duong HTT, Huynh VT, De Souza P, Stenzel MH. *Biomacromolecules*. 2010; 11:2290–2299. [PubMed: 20831272]
- [132]. Soga, O. Thesis. Utrecht university; 2006. p. 87-102.
- [133]. Coimbra M, Rijcken CJF, Stigter M, Hennink WE, Storm G, Schiffelers RM. *J Control Release*. 2012; 163:361–367. [PubMed: 23041274]
- [134]. Talelli M, Oliveira S, Rijcken CJF, Pieters EHE, Etrych T, Ulbrich K, van Nostrum RCF, Storm G, Hennink WE, Lammers T. *Biomaterials*. 2013; 34:1255–1260. [PubMed: 23122804]
- [135]. Quan L, Zhang Y, Crielaard BJ, Dusad A, Lele SM, Rijcken CJF, Metselaar JM, Kostkova H, Etrych TE, Ulbrich K, Kiessling F, Mikuls TR, Hennink WE, Storm G, Lammers T, Wang D. *ACS Nano*. 2013
- [136]. Crielaard BJ, Lammers T, Schiffelers RM, Storm G. *Journal of Controlled Release*. 2012; 161:225–234. [PubMed: 22226771]
- [137]. Etheridge ML, Campbell SA, Erdman AG, Haynes CL, Wolf SM, McCullough J. *Nanomedicine: Nanotechnology, Biology and Medicine*. 2013; 9:1–14.
- [138]. Tinkle S, McNeil SE, Mühlebach S, Bawa R, Borchard G, Barenholz Y, Tamarkin L, Desai N. *Annals of the New York Academy of Sciences*. 2014; 1313:35–56. [PubMed: 24673240]
- [139]. Bissery M-C, Nohynek G, Sanderink G-J, Lavelie F.o. *Anti-Cancer Drugs*. 1995; 6:339–355. [PubMed: 7670132]
- [140]. Crist RM, Grossman JH, Patri AK, Stern ST, Dobrovolskaia MA, Adisheshaiah PP, Clogston JD, McNeil SE. *Integrative Biology*. 2013; 5:66–73. [PubMed: 22772974]
- [141]. Matsumura Y, Kataoka K. *Cancer Science*. 2009; 100:572–579. [PubMed: 19462526]



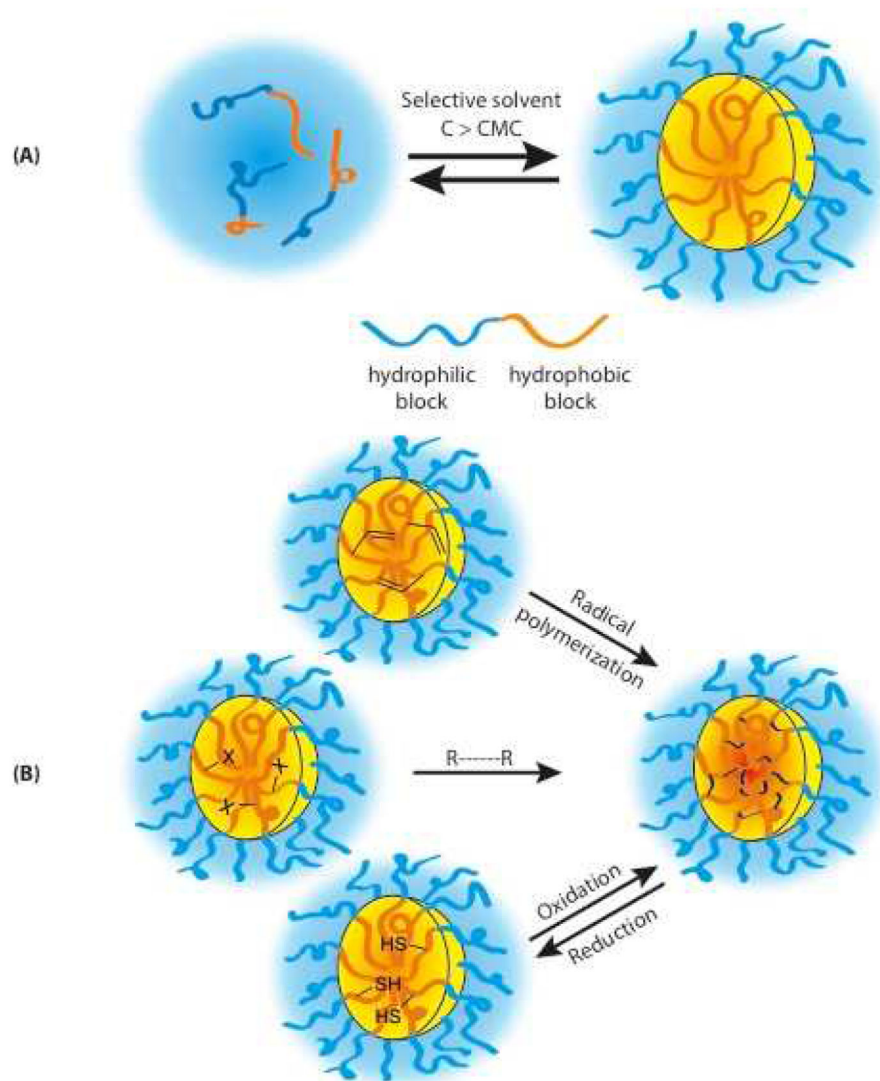
**Figure 1.** Schematic depiction of routinely used nanomedicine formulations. Note that most standard (chemotherapeutic) drug molecules are between 0.1 and 1 nm in diameter.

<p style="text-align: center;"><b>Polymeric micelle (PM)</b></p> 	<ul style="list-style-type: none"> <li>Organized self-assembly composed of amphiphilic macromolecules (amphiphilic, di- or tri-block copolymers) in a block-selective solvent.</li> <li>An ordered micelle is a core-shell structure with a radial density gradient and a maximal radius less than 2 times the contour length of the individual block copolymers it consists of.</li> <li>Micelle formation and stability are concentration-dependent.</li> <li>Polymeric micelles can have low CMC's, but are nonetheless always in equilibrium with individual macromolecules (unimers).</li> <li>Micellar drug formulations tend to enhance bioavailability but fail to change drug pharmacokinetics</li> </ul>
<p style="text-align: center;"><b>Core-crosslinked polymeric micelle</b></p> 	<ul style="list-style-type: none"> <li>Core-shell structure based on amphiphilic block copolymers in which the hydrophobic core is chemically or physically stabilized.</li> <li>Absence of an equilibrium between micelle and unimers.</li> <li>Multiple types of chemical core-crosslinking are possible, e.g. via radical polymerization, via disulfide bridges or via the use of bifunctional agents.</li> <li>They offer the possibility to covalently core-crosslink (pro-) drug molecules, to ensure tailorable release kinetics.</li> <li>Good evidence is available for improved circulation times, increased target site accumulation and enhanced therapeutic efficacy [48, 49].</li> </ul>
<p style="text-align: center;"><b>Core-shell-nanohydrogel</b></p> 	<ul style="list-style-type: none"> <li>A nanohydrogel is defined as a three-dimensional network of hydrophilic polymers in the nanometer range, which expands in the presence of water.</li> <li>Core-shell nanohydrogels possess a core-shell structure, in which the core as well as the shell is hydrophilic.</li> <li>The core is composed of a hydrophilic network and is stabilized either by chemical or physical crosslinks that prevent the particle from dissolution, while the shell is composed of hydrophilic polymer segments.</li> <li>First evidence is available for enhanced circulation times, increased target site accumulation and enhanced therapeutic efficacy [50].</li> </ul>
<p style="text-align: center;"><b>Polymersome</b></p> 	<ul style="list-style-type: none"> <li>Nanovesicles consisting of amphiphilic block copolymers forming a liposome-like bilayer, rather than a core-shell-type micelle.</li> <li>Polymersomes can entrap both hydrophilic (aqueous core) and hydrophobic (lipophilic shell) agents.</li> <li>Stable drug entrapment as well as triggered release is possible by crosslinking of the polymeric bilayer</li> <li>Enhanced <i>in vivo</i> circulation times and target site accumulation have been demonstrated[51].</li> </ul>

**Figure 2.** Definition, schematic structure and general characteristics of self-assembled polymeric core-shell nanomaterials.



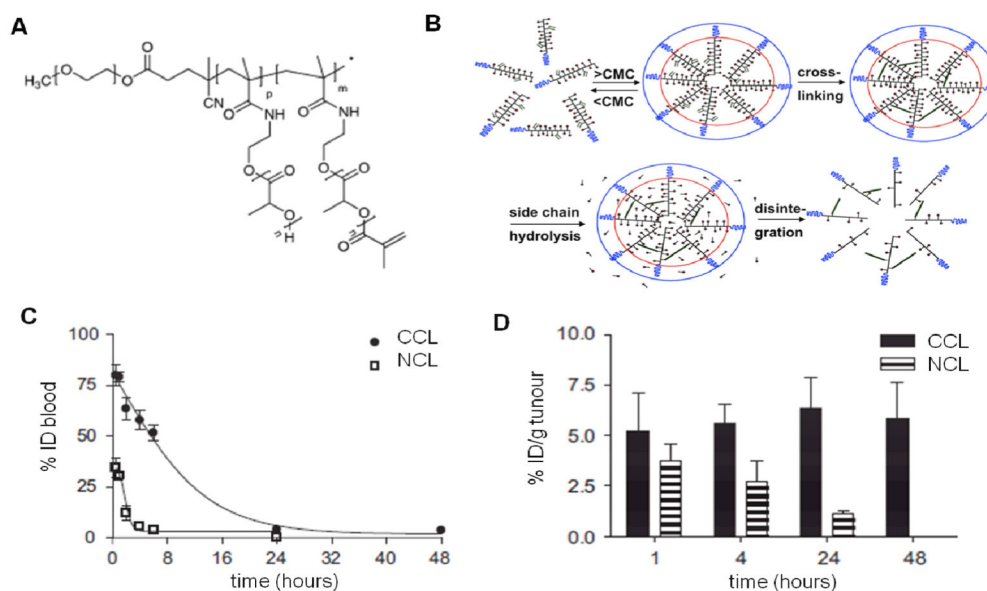
**Figure 3.** Representation of theoretical Gaussian distributions of PHPMA with a degree of polymerisation of 300 ( $M_n = 40$  kg/mol) and relative molar and weight content in different molar mass fractions, in dependence of selected polymer dispersities [56]. Image reproduced from [56] with permission of the Royal Society of Chemistry, Copyright 2011.



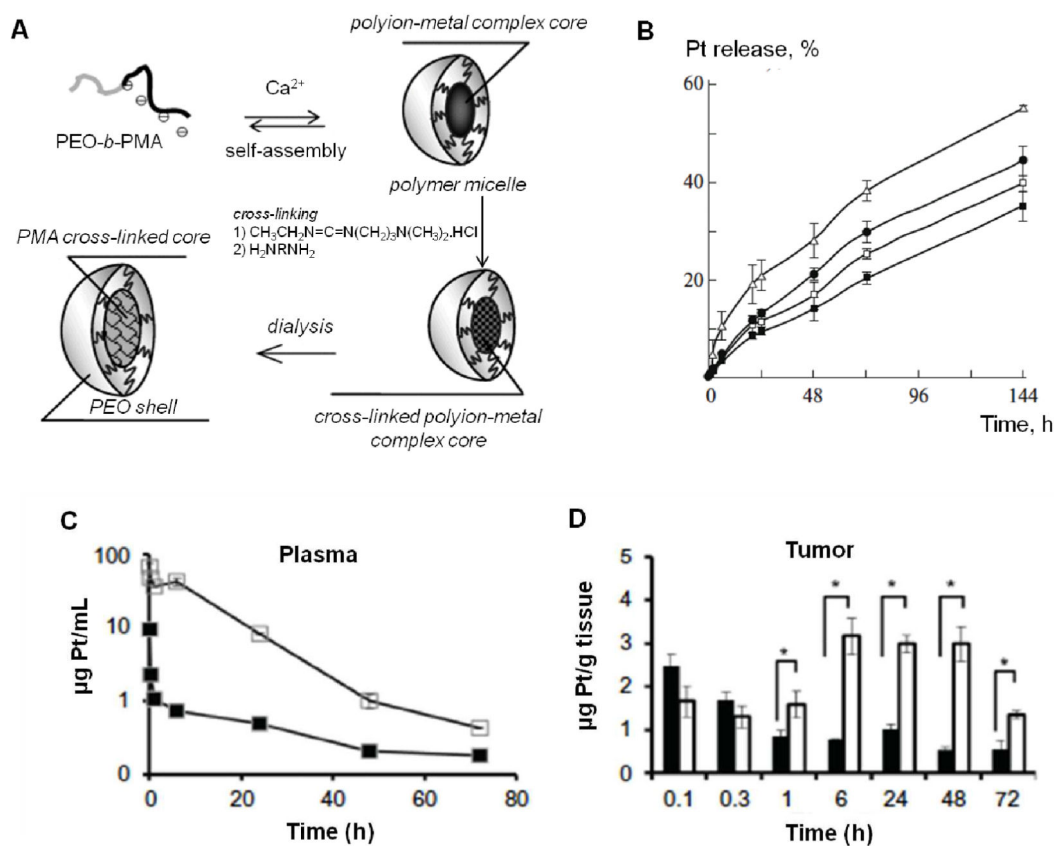
**Figure 4.**

A) Micellization of block copolymers when dissolved in selective solvents at concentrations above the critical micelle concentration (CMC) and B) Methods applied for core-crosslinking of polymeric micelles: I) radical polymerization, used with micelles consisting of polymers containing polymerizable groups, II) bifunctional agents (R---R), used with micelles consisting of polymers containing reactive groups, and III) oxidation of thiols (reversible by reduction), used with micelles consisting of polymers containing thiol groups.

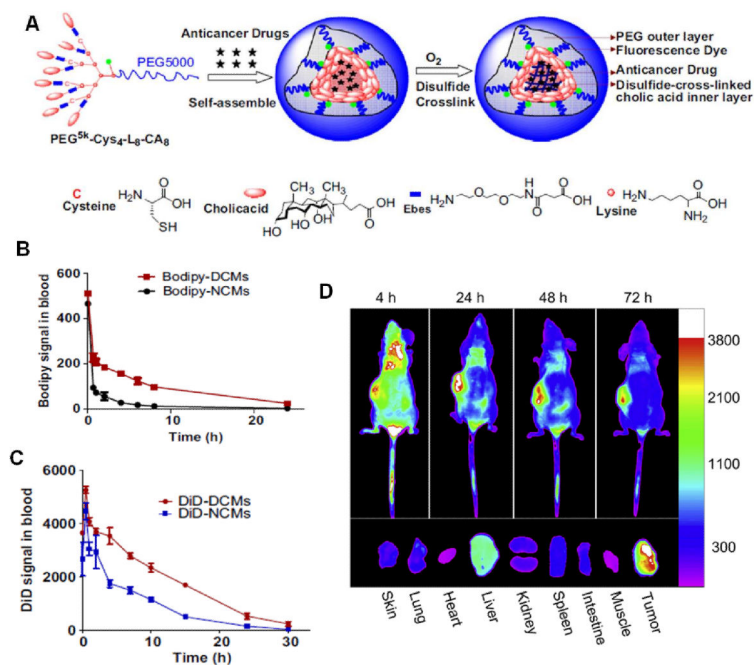


**Figure 5.**

Core-crosslinking of biodegradable polymeric micelles using radical polymerization and its effects on their *in vivo* fate. A) Chemical structure of mPEG-*b*-[N-(2-hydroxyethyl) methacrylamide]-oligolactate] (mPEG-*b*-pHEMAmLac<sub>n</sub>) copolymer with part of the oligolactate side groups methacrylated. B) Formation of micelles based on mPEG-*b*-pHEMAmLac<sub>n</sub> copolymers and subsequent core-crosslinking by free radical polymerization. C) Circulation kinetics and D) tumour accumulation of non-core-crosslinked (NCL) and core-crosslinked (CCL) polymeric micelles in <sup>14</sup>C-tumor bearing mice, evaluated using <sup>3</sup>H-labelled block copolymers [48], convincingly demonstrating significantly improved circulation kinetics and tumor accumulation of the CCPM as compared to NCPM micelles. Image reproduced from [48] with permission of Elsevier, Copyright 2007.

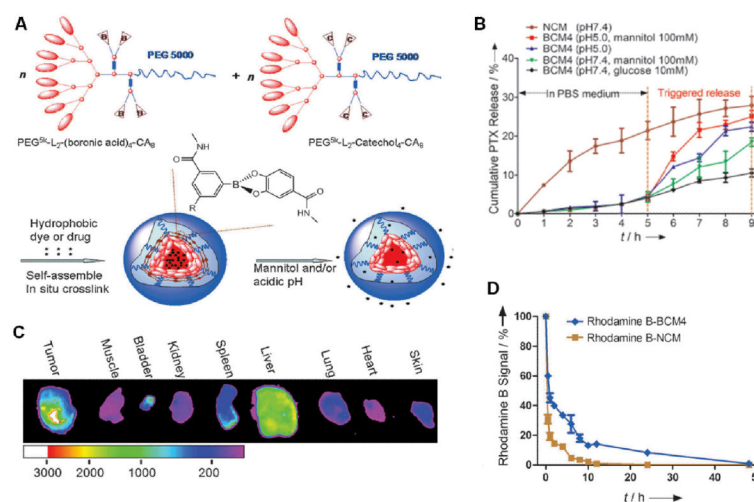


**Figure 6.** Stabilization of block ionomer complex (BIC) micelles by means of core-crosslinking using a diamine. A) BIC micelles based on poly(ethylene glycol)-b-poly(methacrylic acid) (PEG-b-PMA) were core-crosslinked via reaction of the carboxylic groups of PMA with a diamine [104]. B) Sustained cisplatin release from core-crosslinked BIC micelles with different degrees of crosslinking (■—10%, ○—20%, ●—40%, and □—70%) in PBS at pH 7.4 [101]. C) Circulation kinetics of cisplatin upon injection of free cisplatin (■) and cisplatin-loaded CCPM (□) in mice bearing A2780 ovarian carcinoma xenografts [102]. D) Tumor accumulation of cisplatin upon thei.v. injection of free cisplatin (black bars) or cisplatin-loaded CCPM (white bars) in A2780 tumor-bearing mice [102]. Images reproduced from [101] with permission of Springer, Copyright 2009, from [102] with permission of DOVE medical press, Copyright 2012 and from [104] with permission of the American Chemical Society, Copyright 2005.



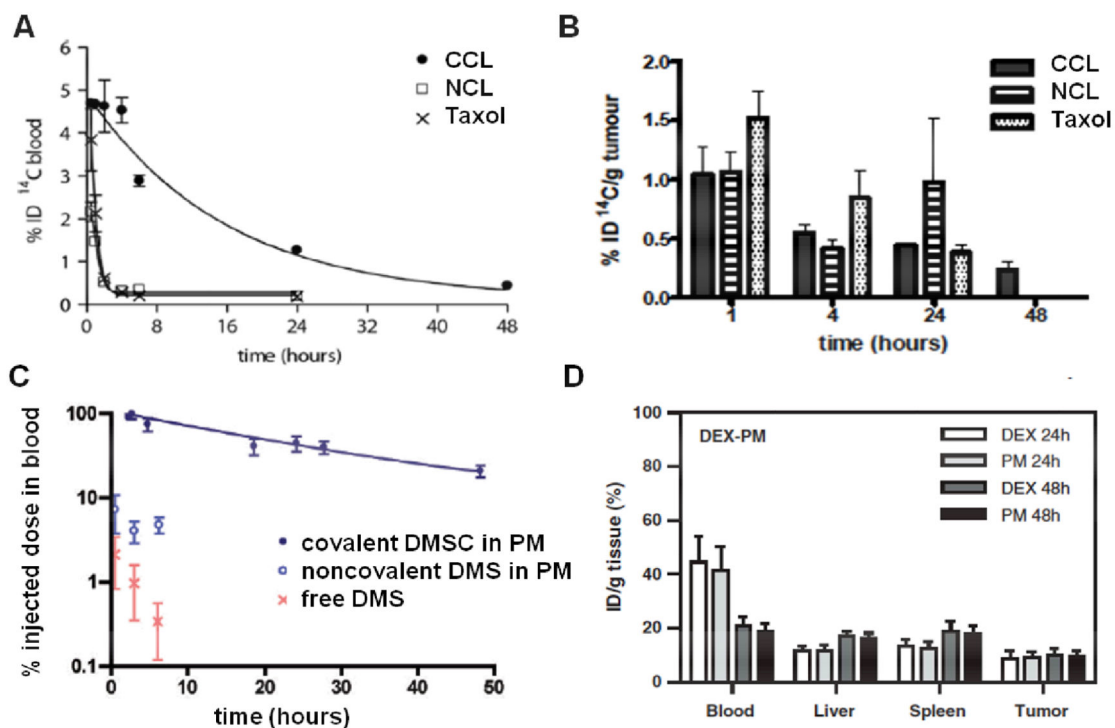
**Figure 7.**

Core-crosslinked polymeric micelles based on thiolated telodendrimers. A) Schematic representation of the self-assembly of PM based on cysteine-containing telodendrimers and their subsequent core-crosslinking by oxidation of the thiol groups. B-C) Circulation kinetics of the BODIPY-labeled micelles (B) and the physically entrapped dye DiD (C) upon i.v. injection in nude mice. The CCPM demonstrated a much better retention of both nanocarrier and model drug in systemic circulation. D) *In vivo* fluorescence reflectance imaging of the biodistribution and the tumor accumulation of the DiD entrapped in CCPM in mice bearing SKOV-3 tumors [120]. Images reproduced from [120] with permission of Elsevier, Copyright 2011.

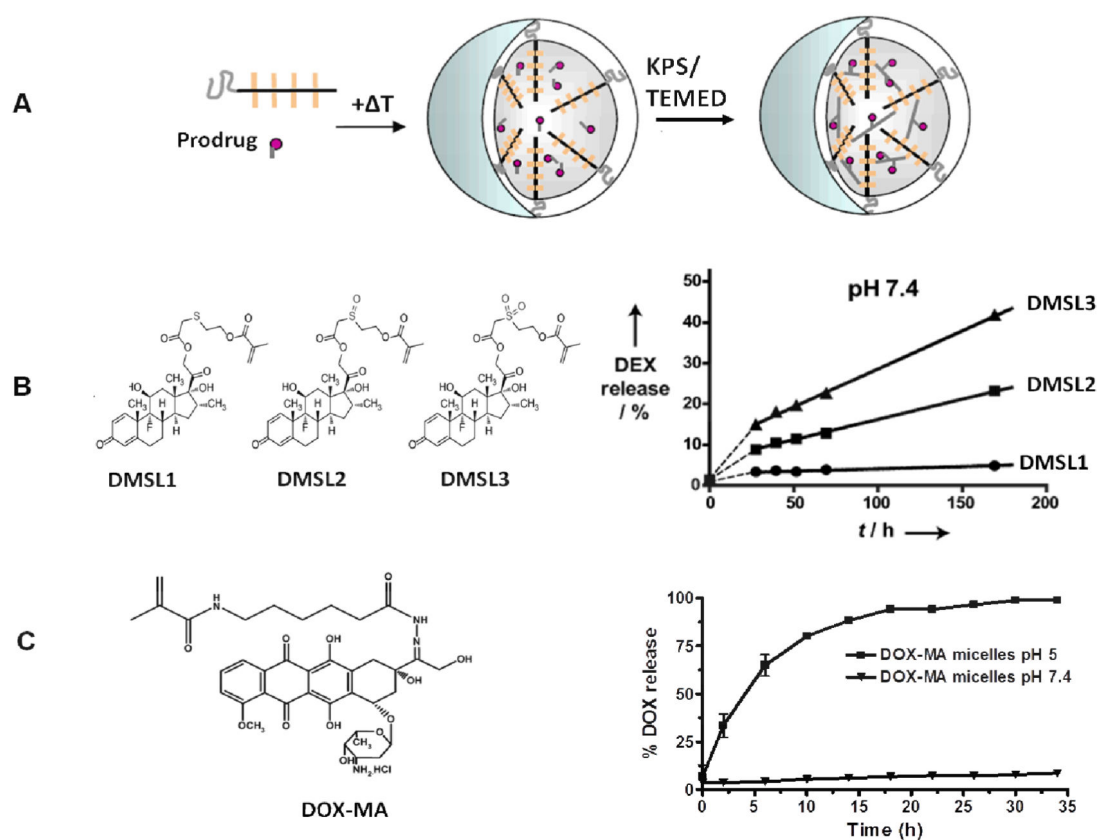


**Figure 8.**

Micelles based on telodendrimers core-crosslinked via boronate esters. A) PEG5000-based dendritic cholic acids were self-assembled into PM and subsequently reversibly core-crosslinked by the formation of boronate esters, which disintegrate in acidic pH or upon the addition of mannitol. B) Stimuli-responsive release of PTX from CCPM and NCPM at acidic pH and upon treatment with mannitol. C) *Ex vivo* fluorescence reflectance imaging of tumors and organs 32 hours after the i.v. injection of DiD-loaded CCPM in SKOV-3 tumor-bearing mice, showing efficient tumor accumulation. D) FRET-based analysis of micelle stability in blood, showing significantly increased rhodamine B signal generation (induced by DiO co-presence in the micellar core) for CCPM [122]. Images reproduced from [122] with permission of Wiley, Copyright 2012.

**Figure 9.**

Effect of covalent vs. physical drug encapsulation in CCPM on the pharmacokinetics and the biodistribution of the drug. A-B: Circulation kinetics (A) and tumor accumulation (B) of  $^{14}\text{C}$ -labeled paclitaxel in free form (Taxol) and loaded in NCPM (NCL) and CCPM (CCL) upon i.v. injection into mice bearing  $^{14}\text{C}$  tumor xenografts [126]. C-D: Circulation kinetics (C) and biodistribution (D) of  $^3\text{H}$ -labeled dexamethasone in free form and covalently or non-covalently entrapped in  $^{14}\text{C}$ -labelled CCPM [41], [133]. Experiments were performed in B16F10-tumor bearing mice. The results clearly show that covalent drug attachment leads to prolonged circulation kinetics (C), and to a biodistributional profile which is very similar for the micelles (PM) and for the drug (DEX), both at 24 and at 48 h post injection (D). Images reproduced from [41] with permission of Walter De Gruyter GmbH, Copyright 2010, and [133] with permission of Elsevier, Copyright 2012.

**Figure 10.**

Prodrugs used for covalent entrapment of therapeutics in the core of CCPM offering tailorable controlled release kinetics. A) Co-crosslinking of methacrylated prodrugs in mPEG-b-pHPMAmLac<sub>n</sub> CCPM by physical entrapment followed by co-polymerization of the methacrylate groups of the prodrug with those of the polymer. B) Methacrylated dexamethasone derivatives containing a sulfide (DMSL1), sulfoxide (DMSL2), or sulfone (DMSL3) ester linker (left), resulting in different release kinetics when covalently entrapped in the core of mPEG-b-pHPMAmLac<sub>n</sub> CCPM (right) [127]. C) Methacrylated doxorubicin derivative (DOX-MA) containing a pH-labile hydrazone linker, resulting in acidic environment-specific release when covalently entrapped in the core of mPEG-b-pHPMAmLac<sub>n</sub> CCPM [49]. Images reproduced from [49] with permission of Elsevier, Copyright 2010, and from [127] with permission of Wiley, Copyright 2012.



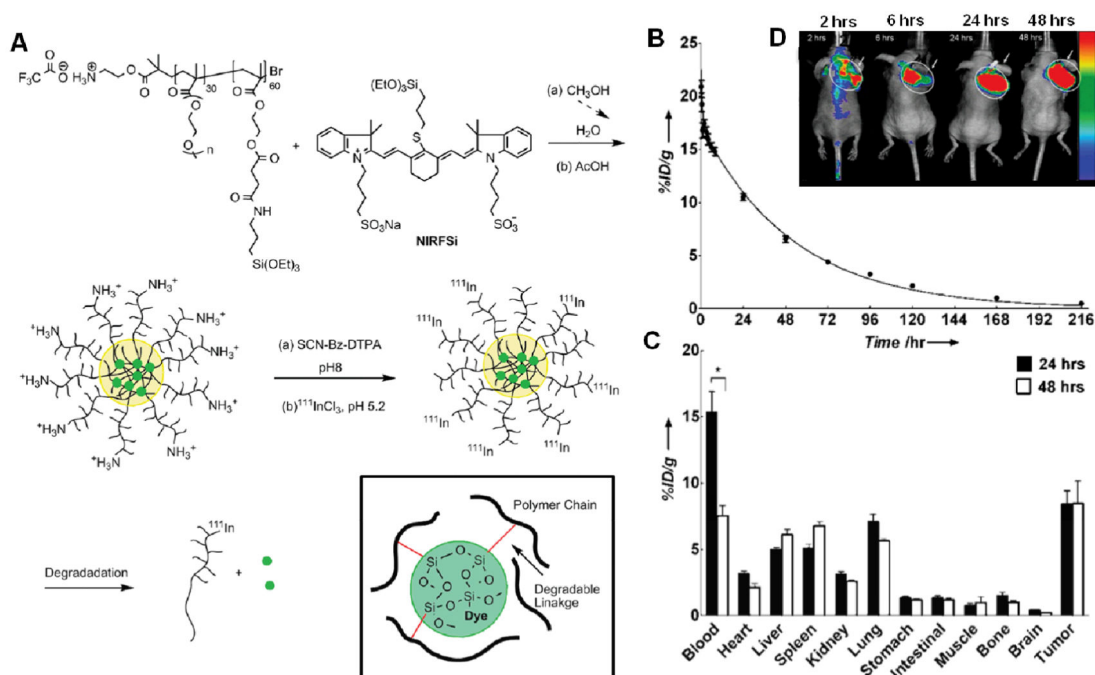


**Figure 11.**

Micelles with ethoxysilane cores loaded with a silane NIRF were core-crosslinked by condensation of the silane groups [124]. A) Synthesis of  $^{111}\text{In}$ -labeled silane core-crosslinked micelles covalently loaded with a silane NIRF, and schematic depiction of their degradation by hydrolysis of the succinic ester linkers in acidic pH, leading to dissociation and model drug release. B) Prolonged circulation kinetics of  $^{111}\text{In}$ -labeled silane CCPM upon injection to Balb/c mice. C) Biodistribution obtained by radioactivity counts of mice bearing CT-26 tumors 24 and 48 hours after the i.v. injection of CCPM, showing increased tumor accumulation at both time points. D) Efficient accumulation and prolonged retention of the covalently attached Cy7-like NIRF (used as a model drug) was observed when optically imaging the biodistribution of the CCPM in CT-26 tumor bearing mice. Images reproduced from [124] with permission of the American Chemical Society, Copyright 2012,.

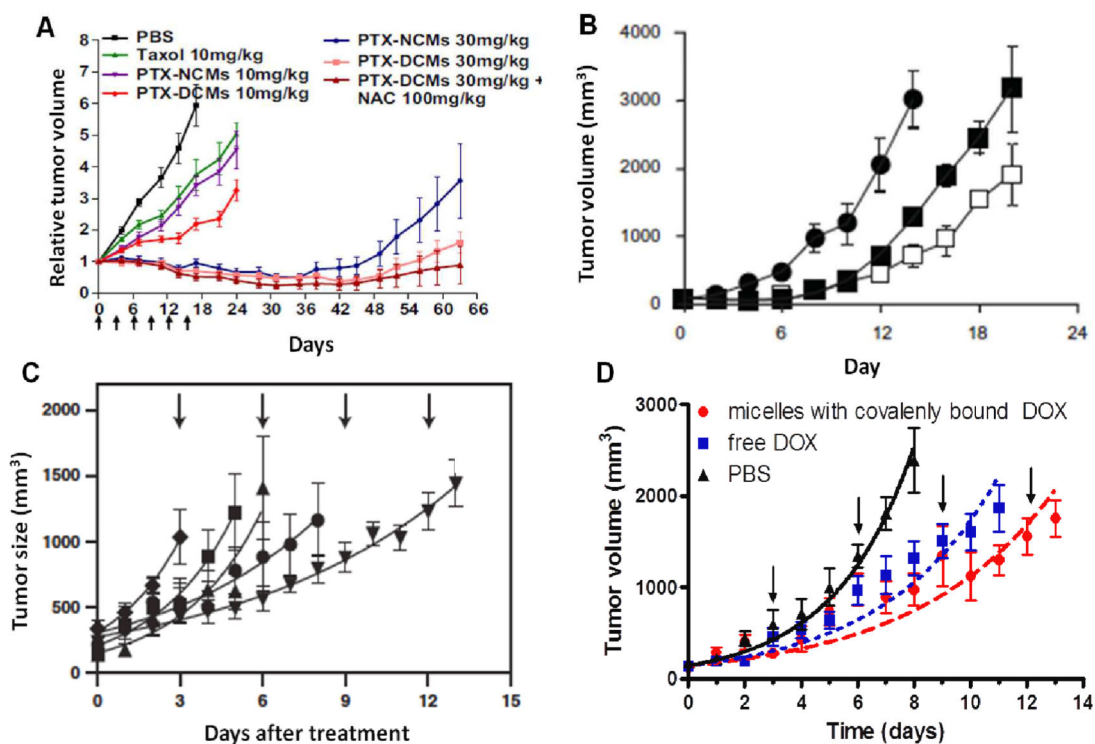


**Figure 12.**

*In vivo* antitumor efficacy of CCPM with physically (A-B) or covalently (C-D) entrapped anticancer agents. A) Tumor growth curves of mice bearing SOV-3 ovarian cancer after treatment with PBS, Taxol, paclitaxel-loaded non-crosslinked micelles (NCM), and paclitaxel-loaded disulphide-core-crosslinked micelles (DCM) based on cysteine-modified telodendrimers [120]. B) Tumor growth in mice bearing A2780 ovarian carcinoma xenografts upon treatment with cisplatin-containing core-crosslinked BIC micelles (□), free cisplatin (■) and solvent (dextrose; ●) [102]. C) Tumor growth in mice bearing B16F10 melanoma tumors after treatment with free dexamethasone (▲), dexamethasone co-crosslinked in the core of CCPM (●), dexamethasone encapsulated in liposomes (▼), unloaded CCPM (■) and PBS (◆) [133]. D) Tumor growth in mice bearing B16F10 melanoma tumors after treatment with PBS, free doxorubicin, and CCPM with covalently entrapped doxorubicin [49]. In all cases, CCPM were more efficient in suppressing tumor growth than control treatments. Images reproduced from [49], [120] and [133] with permission from Elsevier, Copyright 2010, Copyright 2011, Copyright 2012 and from [102] with permission of DOVE medical press, Copyright 2012.

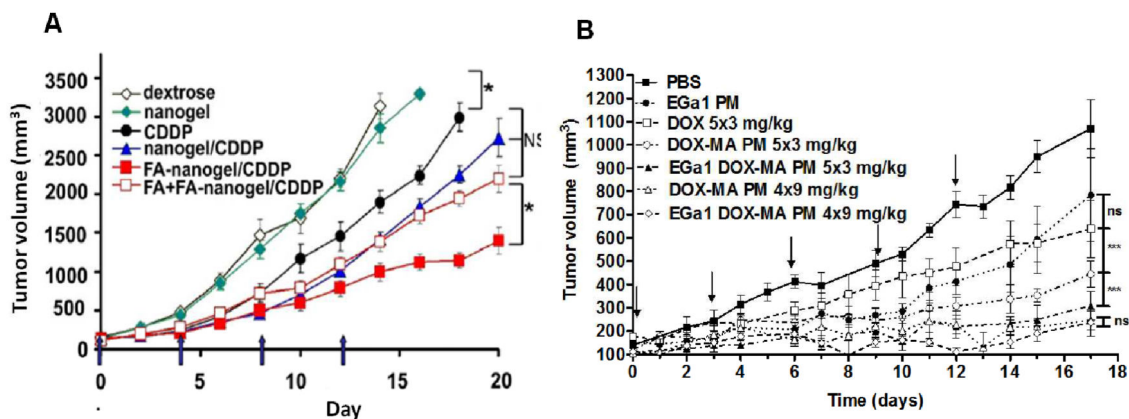


**Figure 13.**

*In vivo* antitumor efficacy of actively targeted CCPM. A) Tumor growth in mice bearing A2780 ovarian tumors after treatment with solvent (dextrose), empty CCPM (nanogel), free cisplatin (CDDP), cisplatin-loaded CCPM, folate-targeted cisplatin-loaded CCPM, and a mixture of folate-targeted cisplatin-loaded CCPM plus free folate (for competition purposes) [107]. B) Tumor growth in mice bearing 14C xenografts upon treatment with empty nanobody-targeted micelles, free doxorubicin, CCPM with covalently attached doxorubicin, and nanobody-targeted CCPM with covalently attached doxorubicin [134]. In both cases, the actively targeted CCPM demonstrated increased tumor growth suppression as compared to the untargeted formulations. Images reproduced from [107] and [134] with permission from Elsevier, Copyright 2011, Copyright 2013.

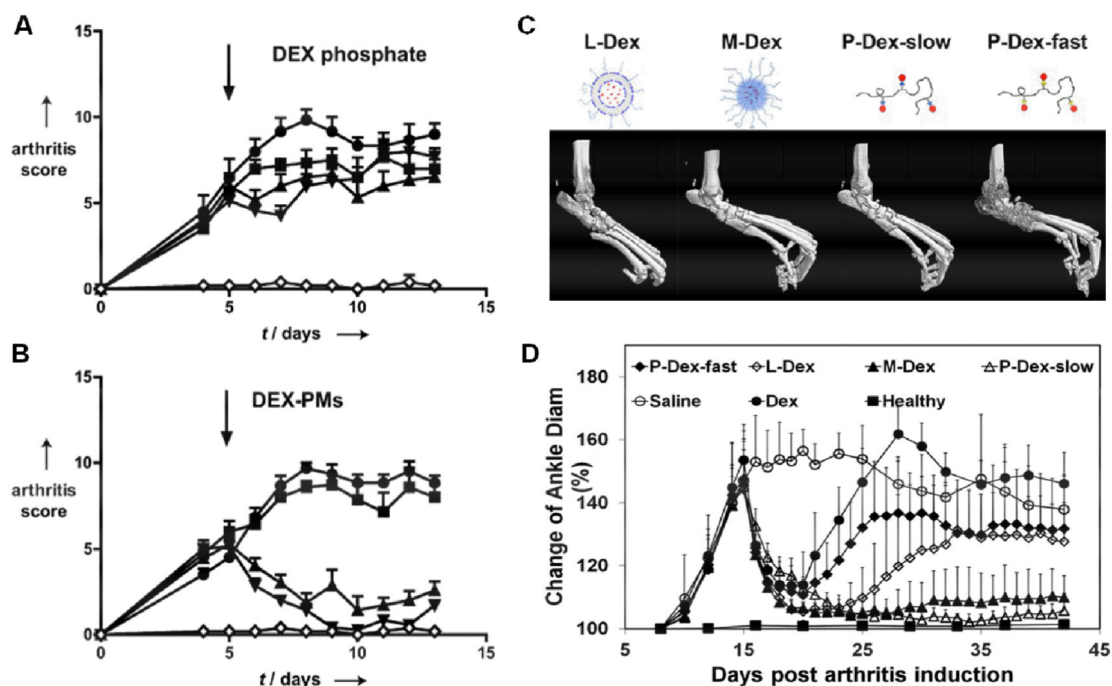


**Figure 14.**

*In vivo* efficacy of CCPM containing covalently entrapped dexamethasone in mice and rats with arthritis. A-B) Therapeutic efficacy of free dexamethasone (DEX; A) and CCPM with covalently attached DEX (B) upon i.v. injection in mice with collagen antibody-induced arthritis, administered at doses of 1 (■), 5 (▲) and 10 (▼) mg/kg of DEX-equivalent [127]. Control mice (●) received PBS (A) or empty micelles (B). Mice without arthritis induction served as healthy controls (◇). C-D) Comparison of the *in vivo* efficacy of four prototypic Dex-containing nanomedicine formulations in rats with adjuvant-induced arthritis. L-DEX: DEX-loaded liposomes. M-DEX: CCPM with covalently entrapped DEX. P-DEX: Slowly or rapidly releasing pHPMA-DEX polymer conjugates [135]. Images reproduced from [127] with permission from Wiley, Copyright 2012 and from [135], with permission from the American Chemical Society, Copyright 2014.

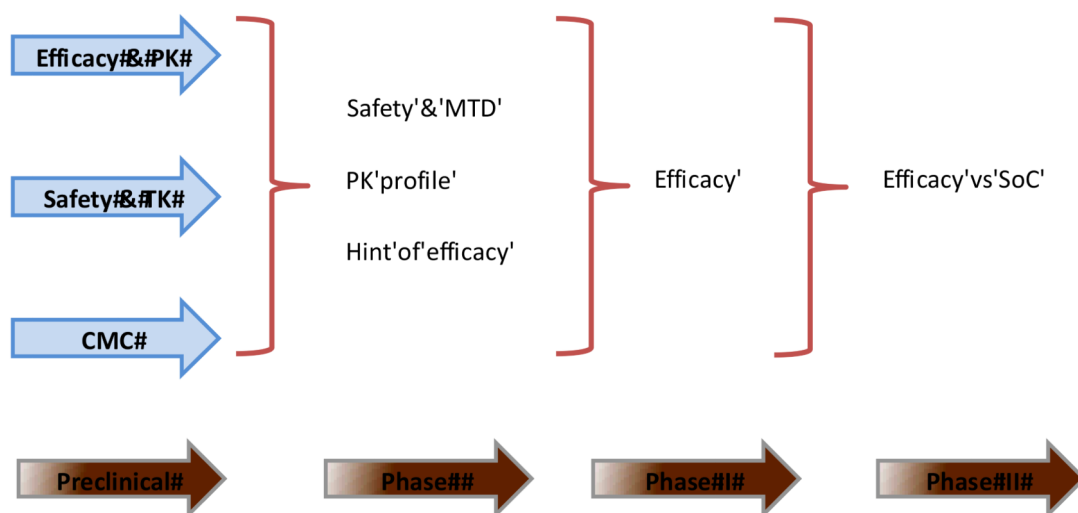


**Figure 15.**

The preclinical to clinical development path of a new chemical entity (NCE; US terminology) or new active substance (NAS; EU terminology) in oncology. PK: pharmacokinetics; TK: toxicokinetics; CMC: chemistry, manufacturing and control; MTD: maximum tolerated dose; SoC: standard of care.

**Table 1**

Selected examples of polymeric micelle formulations that are currently under clinical investigation. mPEG-PDLLA: methoxy-poly(ethylene glycol)-*block*-poly(D, L-lactide), PEG-pAsp: poly(ethylene glycol)-*block*-poly(aspartate), PEG-p(Asp-DOX): poly(ethylene glycol)-*block*-poly(aspartate)-doxorubicin, PEG-P(Glu-SN-38): poly(ethylene glycol)-*block*-poly(glutamate)-SN-38, PEG-pGlu: poly(ethylene glycol)-*block*-poly(glutamate), DACHPt: dichloro(1,2-diaminocyclohexane)platinum(II).

Name	Polymer	Therapeutic	Indication	Phase	Method of entrapment	Size (nm)	Company
<b>Genexol PM</b> [69-72]	mPEG-b-PDLLA	Paclitaxel	Breast, lung, ovarian cancer	Approved	Physical	20-50	Samyang Corporation, South Korea, Sorrento Therapeutics, USA
<b>NK105</b> [40, 73, 74]	PEG-pAsp*	Paclitaxel	Gastric cancer/Breast cancer	III	Physical	85	Nanocarrier/NipponKayaku, Japan
<b>NK911</b> [43, 75]	PEG-p(Asp-DOX)	Doxorubicin	Pancreatic, colorectal cancer	II	Covalent and physical	40	NipponKayaku, Japan
<b>NK012</b> [76, 77]	PEG-p(Glu-SN-38)	SN-38	Breast, lung, colorectal cancer	II	Covalent	20	NipponKayaku, Japan
<b>NC-6004</b> [78, 79]	PEG-pGlu	Cisplatin	Advanced solid tumors	III	Coordination complex	30	Nanocarrier, Japan
<b>NC-4016</b> [80]	PEG-pGlu	DACHPt	Various solid tumors	I	Coordination complex	40	Nanocarrier, Japan
<b>NC-6300</b> [81, 82]	PEG-p(Asp-hydrazone)	Epirubicin	Various solid tumors	I	Covalent	60	Nanocarrier, Japan
<b>SP1049C</b> [39, 83]	Pluronic	Doxorubicin	Advanced adenocarcinoma	II	Physical	30	Supratek, Canada

\* pAsp modified with 4-phenyl-1-butanol.